NJC

Accepted Manuscript

This is an *Accepted Manuscript*, which has been through the Royal Society of Chemistry peer review process and has been accepted for publication.

Accepted Manuscripts are published online shortly after acceptance, before technical editing, formatting and proof reading. Using this free service, authors can make their results available to the community, in citable form, before we publish the edited article. We will replace this *Accepted Manuscript* with the edited and formatted *Advance Article* as soon as it is available.

You can find more information about *Accepted Manuscripts* in the Information for Authors.

Please note that technical editing may introduce minor changes to the text and/or graphics, which may alter content. The journal's standard Terms & Conditions and the Ethical guidelines still apply. In no event shall the Royal Society of Chemistry be held responsible for any errors or omissions in this *Accepted Manuscript* or any consequences arising from the use of any information it contains.

ROYAL SOCIETY OF CHEMISTRY

www.rsc.org/njc

Fluorescence probes for both prokaryotic and eukaryotic cells using new Rhenium (I) tricarbonyl complexes with an electron withdrawing ancillary ligand †

Alexander Carreño[1,2*], Manuel Gacitúa[3], Juan A. Fuentes[4*], Dayán Páez-Hernández[1,2], Juan P. Peñaloza[5], Carolina Otero[5], Marcelo Preite[6], Elies Molins[7], Wesley B. Swords[8], Gerald J. Meyer[8], Juan Manuel Manríquez [9,2], Rubén Polanco[10], Ivonne Chávez[11,2], Ramiro Arratia-Pérez[1,2]

1. Doctorado en Fisicoquímica Molecular, Center of Applied Nanosciences (CENAP), Universidad Andres Bello, República 275, Santiago, Chile
2. Núcleo Milenio de Ingeniería Molecular para Catálisis y Biosensores (MECB), ICM, Chile
3. Center of Applied Ecology and Sustainability (CAPES), Universidad Adolfo Ibáñez, Peñalolén, Chile
4. Laboratorio de Genética y Patogénesis Bacteriana, Facultad de Ciencias Biológicas, Universidad Andrés Bello, República 217, Santiago
5. Center for Integrative Medicine and Innovative Science (CIMIS), Facultad de Medicina, Universidad Andres Bello, Echaurren 183, Santiago, Chile.
6. Departamento de Química Orgánica, Facultad de Química, Pontificia Universidad Católica de Chile, Avenida Vicuña Mackenna 4860, Santiago, Chile
7. Institut de Ciència de Materials de Barcelona (ICMAB-CSIC), Campus de la UAB, 08193-Cerdanyola del Vallès, Barcelona, España
8. Department of Chemistry, Murray Hall 2202B. University of North Carolina at Chapel Hill, USA.
9. Laboratorio de Bionanotecnología, Universidad Bernardo OHiggins, General Gana 1702, Santiago, Chile
10. Centro de Biotecnología Vegetal, Universidad Andres Bello, República 217, Santiago, Chile.
11. Departamento de Química Inorgánica, Facultad de Química, Pontificia Universidad Católica de Chile, Av. Vicuña Mackenna 4860, Macul, Chile.

† Electronic supplementary information (ESI) available.

*** Corresponding author for chemical studies.** acarreno@uc.cl

***Corresponding author for biological studies.** jfuentes@unab.cl

Abstract

Research in fluorescence microscopy presents new challenges, especially with respect to the development of new metal-based fluorophores. In this work, the news *fac*-[$Re(CO)_3$(**bpy**)**L**]PF_6 (**C3**) and *fac*-[$Re(CO)_3$(**dmb**)**L**]PF_6 (**C4**) complexes, where **L** is an ancillary ligand *E*-2-((3-amino-pyridin-4-ylimino)-methyl)-4,6-diterbutylphenol, both exhibiting an intramolecular hydrogen bond, have been synthesized for its use as preliminary probes for fluorescence microscopy. The complexes were characterized using chemical techniques such as UV-Vis, ^{1}H-NMR, TOCSY, FT-IR, cyclic voltammetry, mass spectra (EI-MS 752.22 M^+ for **C3** and 780.26 M^+ for **C4**) and DFT calculations including spin-orbit effects. The electron withdrawing nature of the ancillary ligand **L** in **C3** and **C4** explains their electrochemical behavior, which shows the oxidation of Re^I at 1.84 V for **C3** and at 1.88 V for **C4**. The UV-vis absorption and emission properties have been studied at room temperature in acetonitrile solution. The complexes show luminescent emission with a large Stokes shift (λ_{ex}= 366 nm; λ_{em}= 610 nm for **C3** and λ_{ex}= 361 nm; λ_{em}= 560 nm for **C4**). The TDDFT calculations suggest that an experimental mixed absorption band at 360 nm could be assigned to MLCT (d(Re) →π*(**dmb**)) and LLCT (π(**L**)→π*(**dmb**)) transitions. We also assessed the cytotoxicity of **C3** and **C4** in an epithelial cell line (T84). We found that 12.5 μg/ml of **C3** or **C4** is the minimum concentration needed to kill the 80% of cell population, as determined by neutral red uptake. Finally, the potential of **C3** and **C4** as biological dyes for use in fluorescent microscopy was assessed in bacteria (*Salmonella enterica*) and yeasts (*Candida albicans* and *Cryptococcus* spp.), and in an ovarian cancer cell line (SKOV-3). We found that, in all cases, both **C3** and **C4** are suitable compounds to be used as fluorescent dyes for biological purposes. In addition, we present evidence suggesting that these rhenium (I) tricarbonyl complexes may be also useful as differential fluorescent dyes in yeasts (*Candida albicans* and *Cryptococcus* spp.), without the need of antibodies.

Keywords: Rhenium(I) tricarbonyl, fluorescent microscopy, *Cryptococcus spp*, *Candida Albicans*, SKOV-3

1. INTRODUCTION

Fluorescent probes are essential tools for imaging experiments in fluorescence microscopy. These probes should be excitable with the available light sources and showing high brightness to give rise to contrasted images. In addition, photostability, solubility in aqueous solutions, low cytotoxicity, and small molecular size (relevant for super-resolution imaging) are also high desirable characteristics [1-2]. There exists a variety of currently available fluorophores to choose from, including genetically encoded fluorescent proteins (FPs) [3], quantum dots and nanoparticles [4-5], organic dyes, and metal-based systems (e.g. d^6 complexes) [6-8]. Over the last few years, luminescent d^6 complexes (e.g. Rhenium (I) complexes) have attracted considerable interest for applications in microscopy for biological and biomedical purposes as synthetic fluorescent dyes [9-11]. In particular, their high uptake (lipophilicity), low toxicity and intracellular localization are crucial as imaging agents, thereby the derivatization by different ligands needs to be explored in order to obtain improved d^6 luminescent biomarkers. In particular, Rhenium (I) tricarbonyl complexes with heteroaromatic ligands have been subject of intense investigations with respect to their properties as imaging probes [12-19]. In this class of compounds, *fac*-$Re(CO)_3$(**N,N**)**L** (**N,N**: diimine; **L**: halogen or other ligand in axial position named the ancillary ligand), is the most studied complex because of its photophysical properties, which is closely dependent on the coordinating ligands [20-27]. In this context, the effect of different axial ligands in Rhenium (I) complexes has been explored in several biological imaging experiments, concluding that the choice of the axial ligand is fundamental to control different relevant features [28-30]. With respect to the cell uptake, it has been disclosed that some Rhenium (I) tricarbonyl complexes show an excellent uptake of a human adenocarcinoma cell line, but failed to show good uptake by yeasts, presumably due to the presence of the fungal cell wall [28-29]. This evidence shows that Rhenium (I) tricarbonyl complexes reported so far are suitable for application involving non-walled eukaryotic cells. Furthermore, there are no reports showing Rhenium (I) tricarbonyl complexes as good fluorophores for prokaryotic cells (i.e. bacteria). For these reasons, it becomes evident that Rhenium (I)-based fluorophores must be engineered to efficiently stain fungal cells (i.e. yeasts and other fungi) and prokaryotic microorganisms.

As stated, the study of alternative ancillary ligands is very important to obtain new, improved fluorophores based on Rhenium (I) tricarbonyl complexes. Several studies on biological systems have shown that an intramolecular hydrogen bond (IHB) in amino acids, like histidine, is involved in the electron transport chain by the formation of phenoxy radicals [30-33]. Other bioinspired compounds presenting an IHB have been reported, including dyes in sensitized solar cells [34]. In this context, we have described and alternative and improved synthesis, along with its chemical characterization, of a

Rhenium (I) tricarbonyl complex presenting a Schiff base harboring an IHB [i.e. (E)-2-((3-amino-pyridin-4-ylimino)-methyl)-4,6-di-*tert*-butylphenol (**L**)] as ancillary ligand [35-39]. Furthermore, theoretical evidence using DFT theory taking into account spin-orbit effects, suggests that the IHB also affects the electrochemical response, electronic spectra and luminescent properties in the Rhenium (I) tricarbonyl core [40] and it is crucial to modulate the electronic properties of the complexes, plausibly affecting its features as fluorophores *in vivo*. Despite the promising features of these Rhenium (I) tricarbonyl complexes with Schiff bases harboring an IHB, their potential as fluorophores have not been tested yet in biological systems.

Based on these findings, our group has been exploring new Re (I) complexes with alternative ancillary ligands **L**, potentially suitable as biomarkers. In this work, we report an alternative synthesis of *fac*-$Re(CO)_3$(**bpy**)Br (**C1**) and *fac*-$Re(CO)_3$(**dmb**)Br (**C2**) precursors [41-46], where **bpy** is a 2,2'-bipyridine and **dmb** is 4,4'-dimethyl-2,2'-bipyridine, starting from bromotricarbonyl(tetrahydrofuran)rhenium(I) dimer $(Re(CO)_3Br(THF))_2$ at room temperature [37]. Most importantly, we also report two new Rhenium (I) tricarbonyl complexes of type *fac*-$Re(CO)_3$(**X**)**L** (**C3** and **C4**) where **X** is a **bpy** or **dmb** and **L** is a Schiff base as ancillary ligand, presenting an intramolecular hydrogen bond (Scheme 1). Furthermore, we characterized these two new complexes by FTIR, 1D NMR spectra, cyclic voltammetry, UV-vis and emission spectra. The exchange of the original bromide (in **C1** and **C2**) by the Schiff base **L** (in **C3** and **C4**, respectively) affected some optic and electronic properties. In addition, the oxidation potential of Re (I) to Re (II) is more positive in new Rhenium (I) tricarbonyl complexes compared with their respective precursors, remarking the importance of this ancillary ligand **L** with respect to the modulation of the **C3** and **C4** properties. Furthermore, we found that both **C3** and **C4** had large Stokes shifts, making them attractive candidates for biological imaging applications. Finally, we tested these new Rh **C3** and **C4** complexes regarding their potential as biomarkers to be used as fluorescent probes in confocal microscopy. We found that both **C3** and **C4** were useful to reveal both prokaryotic cells (i.e. the bacterium *Salmonella enterica*) and eukaryotic cells (i.e. the yeasts *Candida albicans* and *Cryptococcus* spp., and the human cell lines SKOV-3 and HEK-293). All these results show that the new Rhenium (I) tricarbonyl complexes (**C3** and **C4**) disclosed in this manuscript are viable alternative compounds to be used as fluorophores for both eukaryotic and prokaryotic cells.

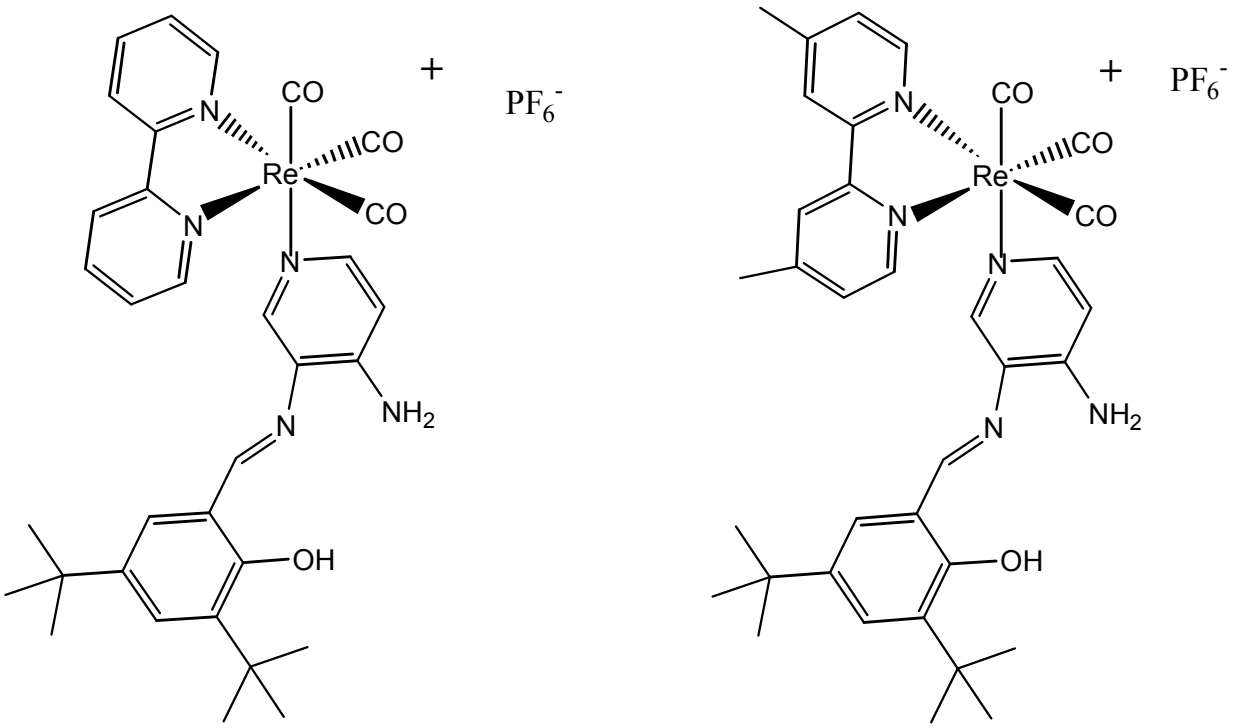

C3 **C4**

Scheme 1. Structures of the *fac*-Re(CO)$_3$(**bpy**)**L**$^+$ (**C3**) and *fac*-Re(CO)$_3$(**dmb**)**L**$^+$ (**C4**) complexes useful as fluorophores for eukaryotic and even prokaryotic cells in confocal microscopy.

2. Experimental Section

2.1 Synthesis. All starting materials were purchased from Merck and Aldrich and used without further purification. The ancillary ligand **L** was synthesized according to literature [35-38]. The methods for preparations of the Rhenium(I) tricarbonyl complexes are given below:

Synthesis of the *fac*-[Re(CO)$_3$(bpy)Br], (C1) complex. The bromotricarbonyl(tetrahydrofuran)rhenium(I) dimer, (5.92×10^{-4} mol) and bipiridyne (**bpy**) (1.18×10^{-3} mol) were added to toluene (25 mL) and stirred for 10 min at room temperature according to literature [37]. The yellow precipitate was collected, and recrystallized from ethanol. Yield 217.5 mg, 87.0 %. ^{1}H NMR (400 MHz, CD_3CN): δ= 7.63 [t, J=6.4 Hz; 1H;H2], 8.19 [d; J=4.6 Hz; 1H;H3], 8.43 [d; J=8.1 Hz; 1H;H4], 9.04 [d; J=5.2 Hz; 1H;H1]. UV/VIS: (acetonitrile, room temperature, c= 5 x 10^{-5} mol L^{-1}) λ(ε)= 292 (5600 mol^{-1} dm^3 cm^{-1}), 383 (2800 mol^{-1} dm^3 cm^{-1}). FTIR (cm^{-1}) 2012; 1903; 1881 (νCO); 1602 (νCC).

Synthesis of the *fac*-[Re(CO)$_3$(dmb)Br], (C2) complex. This complex was synthesized according **C1** procedure. Yield 223.0 mg, 89.0 %. ^{1}H NMR (400 MHz, CD_3CN): δ= 2.41 [s, 3H, ($-CH_3$)], 7.36 [d, J=5.7 Hz; 1H;H2], 8.20 [s, 1H; H3], 8.76 [d, J=5.7 Hz; 1H;H1] . UV/VIS: (acetonitrile, room temperature, c=5 x 10^{-5} mol L^{-1}) λ(ε)= 291 (5600 mol^{-1} dm^3 cm^{-1}), 365 (2800 mol^{-1} dm^3 cm^{-1}). FTIR (cm^{-1}) 2027; 1929; 1907 (νCO); 1590 (νCC).

Synthesis of the *fac*-[Re(CO)$_3$(bpy)(L)](PF$_6$), (C3). To a suspension of **C1** (6.15×10^{-4} mol) in 40 ml of anhydrous THF and Ag(OTf) ($6{,}15\times10^{-4}$ mol) were added under an inert atmosphere in the dark, and left with stirring at room temperature for 2-3 hours. The precipitated AgBr byproduct was removed by filtration, and then the (*E*)-2((3-amino-pyridin-4-ylimino)-methyl)-4,6-diterbutylphenol (**L**) ($6{,}15\times10^{-1}$ mol) was then dissolved in anhydrous THF (30 mL) and added to the previous solution and refluxed for 5 h under a nitrogen atmosphere [46]. The solution was concentrated on a rotary evaporator, and the solid residue dissolved in ethanol. Excess NH_4PF_6 was added, and the mixture was stirred for 12 hours. The solid was precipitated and collected, and recrystallized from ethanol/diethyl ether (1:1, V/V). Yield 172 mg, 86.0%.

^{1}H NMR (400 MHz, CD_3CN): δ= 1.35 [s, 9H], 1.42 [s, 9H], 5.59 [s, 2H, -NH_2], 6.45 [d; J=5.5 Hz; 1H], 7.28 [d; J=1.5 Hz; 1H], 7.43 [s, 1H], 7.51 [s, 1H], 7.53 [s, 1H], 7.77 [dd; 5.5; 7.9 Hz, 2H], 8.11 [s, 1H], 8.28 [dd; J= 5.6; 7.9 Hz; 2H], 8.39 [d; J= 8.3 Hz; 2H], 8.91 [s, 1H], 9.21 [d; J=5.6 Hz; 2H], 12.54 [s, -OH]. UV/VIS: (acetonitrile, room temperature, c= 2.17 x 10^{-5} mol L^{-1}) λ(ε)= 275 (23864 mol^{-1} dm^3 cm^{-1}), 361 (6789 mol^{-1} dm^3 cm^{-1}). FTIR (cm^{-1}): 3407 (νOH); 2871 (νNH_2); 2032 and 1923 (νCO); 1633 (νCN); 845 (νPF_6^-). Elem anal. Calcd for $ReC_{33}H_{35}N_5O_4PF_6$ (896.85): C, 44.20; H, 3.93; N, 7.81. Found: C, 43.73; H, 3.89; N, 7.78. ESI-MS. Calcd (found) for $ReC_{33}H_{35}N_5O_4$: m/z+ 752.22 (752.22).

Synthesis of the *fac*-[$Re(CO)_3$(dmb)(L)](PF_6), (C4). This complex was synthesized according **C3** procedure.Yield 176.0 mg, 88.0%.

^{1}H NMR (400 MHz, CD_3CN): δ=1.36 [s, 9H; -$C(CH_3)_3$], 1.43 [s, 9H; -$C(CH_3)_3$], 5.59 [s, 2H, -NH_2], 6.44 [d, J=6.4 Hz; 1H; H2′], 7.26 [s; 1H; H5′], 7.44 [s, 1H; H3′], 7.55 [s, 2H; H1′], 7.58 [d; J=5.5 Hz; 2H; H2], 8.08 [s, 1H; H4′], 8.24[s; 2H; H3], 9.03 [d; J=5.5 Hz; 2H; H1], 12.55 [s; 1H; -OH]. UV/VIS: (acetonitrile, room temperature, c= 2.17 x 10^{-5} mol L^{-1}) λ(ε)= 275 (23 864 mol^{-1} dm^3 cm^{-1}), 361 (6 789 mol^{-1} dm^3 cm^{-1}). FTIR (cm^{-1}): 3407 (νOH); 2871 (νNH_2); 2027 and 1929 (νCO), 1623 (νCN); 847 (νPF_6-). Elem anal. Calcd for $ReC_{35}H_{39}N_5O_4PF_6$ (925.22): C, 45.45; H, 4.25; N, 43.80. Found: C, 43.80; H, 4.20; N, 7.55.ESI-MS. Calcd (found) for $ReC_{35}H_{39}N_5O_4$: m/z+ 780.26 (780.26).

2.2 Characterization

The NMR spectra were recorded on a Bruker AVANCE 400 spectrometer at 25 ºC. Samples were dissolved in deuterated acetonitrile, using tetramethylsilane as an internal reference. IR spectra were obtained on a Perkin-Elmer 1310 or in a Bruker Vector-22 FT-IR spectrophotometer, in KBr discs. UV-vis absorption spectra for **C3** and **C4** were recorded using a Varian Cary 60 UV-vis spectrophotometer with a resolution of 1nm. Steady-state photoluminescence spectra were measured on an ISS K2 fluorimeter. Samples in acetonitrile were sparged with solvent saturated argon for 30 minutes and excited at $\lambda \approx 445$ nm. The intensity was integrated for 0.5 seconds with 2 nm resolution. PL quantum yields were measured through comparative actinometry using $[Ru(bpy)_3][PF_6]_2$ in acetonitrile (Φ_{em} = 0.06) as a quantum yield standard. [47] Photoluminescence lifetime measurements were performed on was a PTI nitrogen dye laser with excitation centered around 445nm. Decays were monitored at the PL maximum and averaged over 180 scans.

For the electrochemical experiments, the working solution contained 1.0×10^{-2} mol L^{-1} of **C1, C2, C3** and **C4** complexes with 1.0×10^{-1} mol L^{-1} of tetrabutylammonium hexafluorophosphate ($TBAPF_6$) as supporting electrolyte in anhydrous CH_3CN (ACN). Prior to each experiment the solution was purged with high purity argon, and an argon atmosphere was maintained over the solution during the whole experiment. A polycrystalline non-annealed platinum disc (diameter 2 mm) was used as working electrode. As counter electrode, a platinum gauze of large geometrical area was employed, separated from the cell main compartment by a fine grain sintered glass. All potentials quoted in this text refer to an Ag|AgCl electrode in tetramethylammonium chloride to match the potential of a saturated calomel electrode (SCE) at room temperature. All electrochemical experiments were performed at room temperature on a CHI900B bipotentiostat interfaced to a PC running the CHI 9.12 software that allowed experimental control and data acquisition. Elemental Analysis was performed by Atlantic Microlab, Inc. Mass spectra samples were analyzed with a hybrid LTQ FT (ICR 7T) (ThermoFisher, Bremen, Germany) mass spectrometer. Samples were introduced via a micro-electrospray source at a flow rate of 3 μL/min. A total of 300 scans (0.5 sec transients) were averaged for each sample. Xcalibur (ThermoFisher, Breman, Germany) was used to analyze the data. Molecular formula assignments were determined with Molecular Formula Calculator (v 1.2.3). Low-resolution mass spectrometry (linear ion trap) provided independent verification of molecular weight distributions. All singly charged species were verified by unit *m/z* separation between mass spectral peaks corresponding to the ^{12}C and $^{13}C^{12}C_{c-1}$ isotope for each elemental composition. The unique metal isotope signatures provided additional isotope confirmation.

2.3 Computational details

All structural and electronic properties of **C4** were obtained using the Amsterdam Density Functional (ADF) code. [48] The molecular structures were fully optimized by an analytical energy gradient method as implemented by Verluis and Ziegler, [49-50] using the PBE functional [51] and the standard Slater-type-orbital (STO) basis set with triple-ζ quality double plus polarization functions (TZ2P) for all the atoms. Frequency analyses were performed after the geometry optimization to corroborate the minimum configuration. Solvation effects were simulated by the Conductor-like screening model (COSMO) using acetonitrile (CH_3CN) as the solvent, since this solvent was used in the UV-vis and cyclic voltammetry measurements.

2.4 Cytotoxicity assessed by neutral red uptake

Cytotoxicity of *fac*-Re(CO)$_3$(**bpy**)**L(PF$_6$)** (**C3)** or *fac*-Re(CO)$_3$(**dmb**)**L(PF$_6$)** (**C4)** towards an epithelial cell line (T84) was assessed by a modification of the neutral red uptake assay. T84 cells were cultured as previously described. [52] When cells were confluent, monolayers were washed twice with sterile PBS. One volume of **C3** or **C4** (400 ppm in DMSO) was mixed with one volume of cell culture medium (1:1 v/v), and different dilutions were placed on the cells prior to incubate 24 h at 37 °C. Cells were washed twice with PBS, and cell culture medium supplemented with 60 µg/ml of neutral red was added prior to incubating 1.5 h at 37 °C. Cells were washed twice with PBS and destaining solution (50% ethanol 96%, 49% deionized water, 1% glacial acetic acid) was added to cells. Cells were incubated 5 min at room temperature and absorbance at 540 nm was measured. Low absorbance (i.e. low neutral red uptake) is correlated with higher cytotoxicity (or lower cell viability).

2.5 Fluorescence microscopy studies

Bacteria (*Salmonella enterica* serovar Typhimurium ATCC14028s) were grown at 37 °C in Luria-Bertani broth to OD_{600} = 1.4 (stationary phase) with shaking. Yeasts (*Candida albicans* and *Cryptococcus* spp.) were grown in Sabouraud agar at 28 °C. For staining, either bacteria or yeasts (approximately 10^9 cfu/ml) were washed twice and resuspended in one volume of phosphate buffer solution (PBS). The microorganisms were mixed with one volume of *fac*-Re(CO)$_3$(**dmb**)**L(PF$_6$)** (**C3)** or *fac*-Re(CO)$_3$(**dmb**)**L(PF$_6$)** (**C4)** (400 ppm in DMSO), incubated 5 min at 37 °C and subsequently washed three times with PBS to remove the excess of **C3** or **C4**. Finally, microorganisms were suspended again in one volume of PBS prior to being observed fresh at 100X with the confocal microscopy. Fluorescence emission was obtained by laser excitation at 405 nm for both **C3** and **C4**. Emission was collected with a long-pass emission filter in the range of 535 to 655 for the two rhenium (I) complexes. For the autofluorescence, the excitation was 405 nm, and the emission was in the range of 454 and 504 nm. [39]

Human ovarian adenocarcinoma cell line (SKOV-3) was grown in Dulbecco's Modified Eagle's Medium (DMEM) supplemented with 10% v/v fetal bovine serum and 1% penicillin-streptomycin solution (HyClone™, South Logan, Utah, USA). Cells were incubated at 37°C and 5% CO_2. Staining of rhenium complexes was evaluated by fluorescence microscopy. Cells were seeded on 24-well plates in coverslips and incubated for 24 h. Then, cells were washed twice with PBS and concentrated stock solution in DMSO of *fac*-Re(CO)$_3$(**bpy**)**L(PF$_6$)** (**C3)** and *fac*-Re(CO)$_3$(**dmb**)**L(PF$_6$)** (**C4)** were diluted with cell culture medium to final concentration of 50 µM and incubated for 24 and 48 h. Total amount

of DMSO in the dilutions used was under 0.5% in every case in order to ensure full cell viability. After incubation time, cells were washed twice with PBS and fixed for 10 min with 4% paraformaldehyde followed by three washing steps with PBS. Additionally, cells were incubated with Hoechst 33342 as nuclei marker. Finally, cells were mounted on glass slides using Fluoromount-G (Electron Microscopy Sciences, Hatfield, Pennsylvania, USA). Fluorescence was analyzed by a fluorescent microscope Olympus BX63 (Shinjuku, Tokyo, Japan) using a filter system consisting of an excitation between 330 and 385 nm and a long-pass emission filter for wavelengths higher than 420 nm for detection [53-54].

3. Results and Discussion

3.1 Synthesis and characterization

The structures of *fac*-Re(CO)$_3$(**dmb**)**L**$^+$ (**C3**) and *fac*-Re(CO)$_3$(**dmb**)**L**$^+$ (**C4**) complexes were shown in Scheme 1. Complexes *fac*-Re(CO)$_3$(**bpy**)**Br** (**C1**) and *fac*-Re(CO)$_3$(**dmb**)**Br** (**C2**) were previously published, and their synthesis was perfomed by the traditional route [55-57]. In this work, **C1** and **C2** were prepared by reacting bromotricarbonyl(tetrahydrofuran)rhenium (I) dimer as described [37]. The synthesis of (*E*)-2-((3-amino-pyridin-4- ylimino)-methyl)-4,6-diterbutylphenol **L** was previously reported by Kleij *et al*. [35-36] and its electronic, biological and others properties were reported by Carreño *et al*. [37-38]

Rhenium(I) tricarbonyl complexes with the following general configuration [Re(CO)$_3$(X)L] possess Cs, symmetry, with three infra-red (IR) active modes [A'(l) + A'(2) + A"] [58-59]. This pattern corresponds to three carbonyls in a facial (*fac*) isomer arrangement. The ν_{CO} bands appear at 2012 cm^{-1}, 1903 cm^{-1} and 1881 cm^{-1} for **C1,** and at 2027 cm^{-1}, 1929 cm^{-1} and 1907 cm^{-1} for **C2** (The CO bands were assigned to the A'(l), A" and A' (2) vibrations, respectively). There is no evidence in the literature for the formation of Rhenium(I) tricarbonyl complexes in a meridional (mer-) isomeric form of type [Re(CO)$_3$(X)L] with X in bidentate ligands (such as bpy or similar). Rhenium tricarbonyl complexes where X is a monodentate ligand like phosphine such as mer-trans-bromo-tricarbonyI-bis(diphenyl-methyl- phosphÍnite)rhenium(I), presents meridional isomeric form had been reported.[60] A characteristic properties of mer-isomers is the very low IR intensity of the highest frequency band with respect to the other two bands, which is not observed for **C1** and **C2**.

In the case of **C3** and **C4** (See Figure S1 and S2 in the ESI†) only two bands were observed due to the local symmetry loss at 2032 cm^{-1} and 1933 cm^{-1} for **C3,** and at 2027 cm^{-1} and 1929 cm^{-1} for **C4.** These values for the CO vibrational bands indicated that metal back bonding effects are acting since these values are smaller than free ν(CO). This result suggests an Re-C bond lengthening and C-O bond shortening [37]. In addition, a stretching signal observed at 911 cm^{-1} for **C3** and 847 cm^{-1} for **C4** were assigned to the PF_6^- anion. The azomethine stretching (–CH=N-) in the free ligand **L** was located at 1612 cm^{-1} [38] and for the complexes at 1633 cm^{-1} for **C3** and 1623 cm^{-1} for **C4**.

Elemental analysis and mass spectra analysis are in good agreement. The ESI mass spectrum of **C3** (see Fig. S3 in the ESI†) showed a major fragment at m/z = 752.22 and **C4** (see Fig. S4 in the ESI†) at m/z = 780.26 in agreement with the expected value for the molecular ion (It aligns with the Re^{+} complex without the PF_6^{-}). For both compounds **C3** and **C4** the isotope structure is consistent with Rhenium composition.

On the other hands, single crystals of *fac*-$Re(CO)_3$(**dmb**)**L**(**PF_6**) (**C4**) were obtained by slow evaporation of a dichloromethane solution at room temperature, yielding small yellow blocks. A preliminary crystal structure elucidation obtained from a reduced data set at room temperature confirmed the molecular structure. [61] The crystal structure of **C4** showing a *fac*- correlation of the three carbonyl ligands according to the observed by FTIR spectra. The coordination is completed by the **dmb** ligand in the equatorial plane and an axial (*E*)-2-((3-amino-pyridin-4-ylimino)-methyl)-4,6-diterbutylphenol (**L**) ligand resulting in a octahedral geometry. The first step in the theoretical calculations was a geometry optimization of the **C4** compound. The geometrical parameters in the **C4** structure shows the following important bonding distances: Re1-C24 at 1.93 Å; Re1-N1 at 2.23 Å and Re1-N4 at 2.17 Å, respectively. The dihedral angle between the metal and the carbonyl group (C25-Re1-C26) is 89.2 º, in good agreement with similar compounds. [62] The DFT optimized structure of **C4** is shown in figure 1.

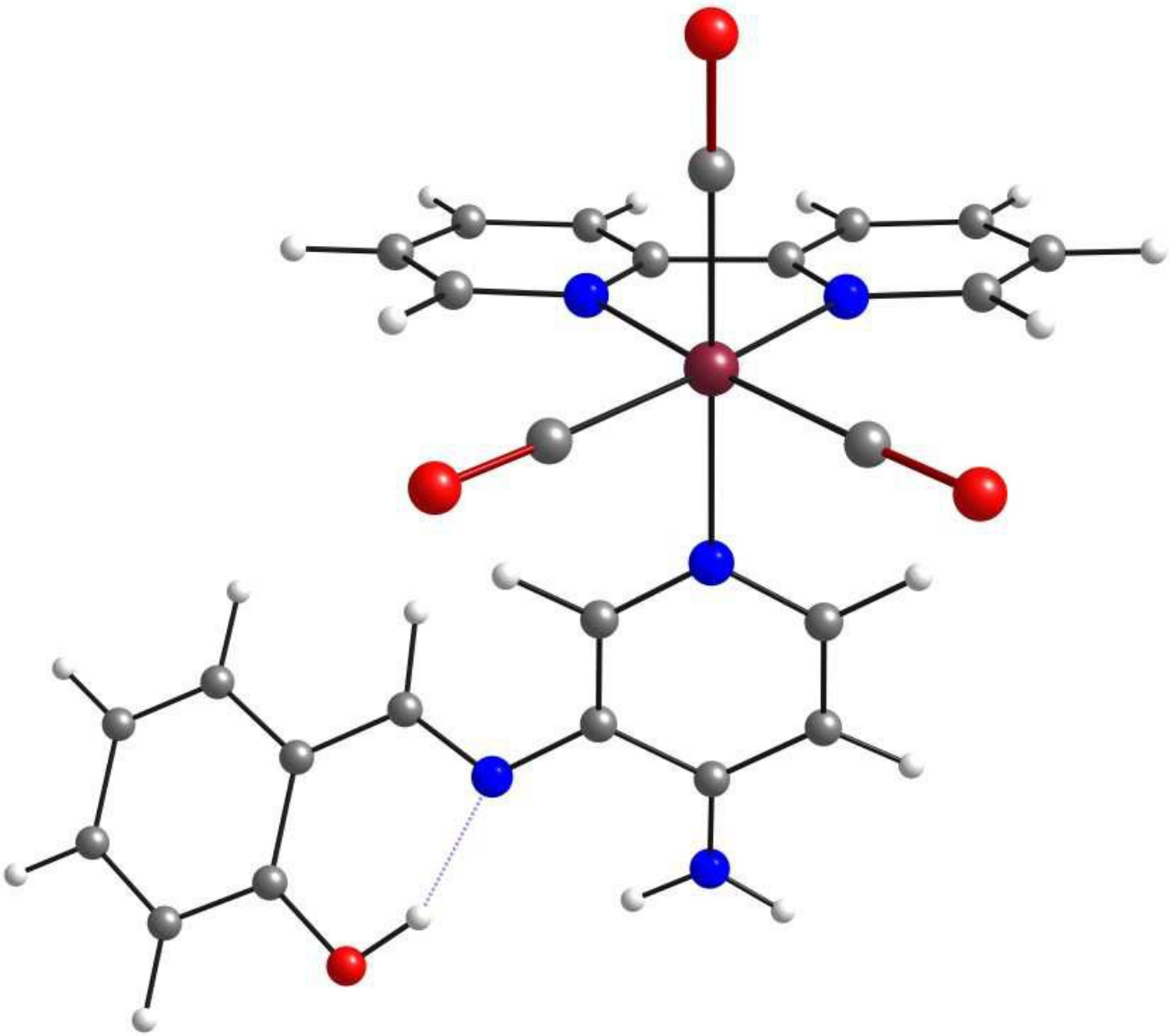

Figure 1. DFT optimized structure of **C4** (tert-butyl groups in **L** and the methyl group in **dmb** have been eliminated for simplicity).

Following with the characterization, the ^{1}HNMR spectrum for (*E*)-2((3-amino-pyridin-4-ylimino)-methyl)-4,6-diterbutylphenol (**L**) ligand exhibits an important peak at approximately 13.0 ppm which was assigned to –OH groups, as previously reported for similar compounds and described in our previous reports. [37-38] On the other hand, the equivalence of the proton peak signals in the ^{1}HNMR spectra for **C1** and **C2** (Numbering of protons are provided in the Figures S5 to S8 in the ESI†) indicated the symmetrical nature of the **bpy** and **dmb** ligands in both complexes. [63-64]

^{1}HNMR spectra were obtained in acetonitrile-d_6 solutions for determined the structure of **C3** and **C4**. After formation of the **C3** and **C4** complexes, the ^{1}HNMR shows changes in the chemical shift relative to the **bpy** or **dmb** and **L** ligands. The aromatic proton resonances from the **bpy** and **dmb** ligands showed shifs to lower values of field compared to the corresponding **C1** and **C2** precursors (see Figures S9 and S10 in the ESI†).

By contrast, the signals attributed to the (*E*)-2((3-amino-pyridin-4-ylimino)-methyl)-4,6-diterbutylphenol (**L**) ancillary ligand suffer displacements to higher fields in both complexes. The important signal associated to the presence of the –OH groups appears at 12.5 ppm; this effect was analyzed in our previous reports where was related to the presence of intramolecular hydrogen bonds between the ligands **L** and neighboring Rhenium(I) tricarbonyl complexes. After the addition of D_2O, the signals disappear from the spectrum in both compounds (**C3** and **C4**), which corroborate our assignment (data not shown).

To complete the assignment, the TOCSY spectrum allowed us to identify the resonances for all protons of **bpy** or **dmb** in the **C3** and **C4** complexes. When irradiating the assigned H1 at 9.24 ppm in **C3** (see Figure S11 in the ESI†), an enhancement were observed for H2 (7.81 ppm), H3 (8.31 ppm) and H4 (8.43 ppm), respectively. In the same manner, when H4 (see Figure S12 in the ESI†) was irradiated, a spectrum showing enhancement for H1, H2 and H4 were obtained. When H3 was irradiated instead (see Figure S13 in the ESI†); H1, H2 and H4 signals were observed. The same form for **C4**, when H1 was irradiated (see Figure S14 in the ESI†), an enhancement were observed for H2 (7.61 ppm) and H3 (8.28 ppm) and the -CH_3 signals were observed. Similarly, we observed the same effect when H3 was irradiated (see Figure S15 in the ESI†). These experiments allowed us to assign all signals to their respective protons of **bpy** or **dmb** and **L** ligands in the **C3** and **C4** complexes.

The UV-vis spectra in acetonitrile were recorded at room temperature for **C1** and **C2** and showed two absorption bands which were assigned to $\pi\rightarrow\pi^*$ and MLCT transition at 292 nm (5.6 x 10^3 dm^3 mol^{-1} cm^{-1}) and 383 nm (2.8 x10^3 dm^3 mol^{-1} cm^{-1}) for **C1** and at 291 nm (ε= 5.6 x 10^3 dm^3 mol^{-1} cm^{-1}) and 365 nm (ε= 2.8 x10^3 dm^3 mol^{-1} cm^{-1}) for **C2** according to literature. [65-67]

In the case of **C3** and **C4** complexes, two blue-shifted absorption bands can be appreciated at 275 nm and 366 nm for **C3** and 274 nm and 361 nm for **C4**. The first one corresponds to the π→π* intraligand transition, while the second one is assigned to a metal to ligand charge tranfer (MLCT) transition and an interligand charge transfer transition (LLCT). Thus, the blue shift observed and is attributed to the electron withdrawing nature of (*E*)-2((3-amino-pyridin-4-ylimino)-methyl)-4,6-diterbutylphenol (**L**) ancillary ligand, which was reported previously. [37]

To completed these study, DFT calculations including scalar and SO relativistic effects. As the SO effect is included, double group irreducible representation (irreps) need to be used, where the high occupied molecular orbitals (HOMO) were transformed to the highest occupied molecular spinor (HOMS). In **C4** the HOMS is located mainly over the (*E*)-2((3-amino-pyridin-4-ylimino)-methyl)-4,6-diterbutylphenol (**L**) ancillary ligand, and corresponds to the π deslocalized orbital of **L**. On the other hands, HOMS-1 is again a π orbital but now has a large contribution of dπ(Re). On the other hand, the orbitals from LUMS to LUMS+2 are centered on the **dmb** ligand and LUMS+3 has a π* character centered around pyridine and phenol rings on the **L** ligand. [37]

The calculated vertical electronic transitions for **C4** in acetonitrile as solvent, show two important transition; the one at 360 nm which represent a mixing between π(**L**) → π*(**dmb**) and d(Re) → π*(**dmb**) transitions with LLCT and MLCT characters respectively (see Table 1 and figure 2). The transition at 269 nm corresponding to d(Re) → π*(**dmb**) with MLCT characters. These two calculated transitions are in good agreement with the experimental values. These is consistent with the previous results of Sacksteder *et al.* [40] who verified the dependence of the acceptor/donor abilities of ancillary ligands in the properties of the Rhenium(I) tricarbonyl core.

On the other hand, **C4** showed important differences in the electronic energy levels due to the change of the ancillary ligand. Bromide in **C2** has electron donating ability compared with the (*E*)-2((3-amino-pyridin-4-ylimino)-methyl)-4,6-diterbutylphenol (**L**) ancillary ligand in **C4**, which shows electron withdrawing ability. This change causes a narrow electronic transition energy gap that was described in literature [37]. Furthermore, Liu *et al*. have reported earlier that the LUMO energy is also affected by the nature of the ancillary ligand, showing in other complexes the stabilization in energy of the LUMO due to the introduction of an electron withdrawing ligand. [68]

Table 1. Calculated absorption bands for **C4** compound.

λ calc	**f (x 10^{-2})**	**Assignment**
269	2.1	100% HOMS-3→LUMS+7 d(Re) →π* (**dmb**)
360	9.8	60% HOMS-5→LUMS+2 π(**L**) → π*(**dmb**) 40% HOMS-3→LUMS+2 d(Re) →π*(**dmb**)
388	1.9	100% HOMS-3-LUMS+3 d(Re) →π*(**L**)

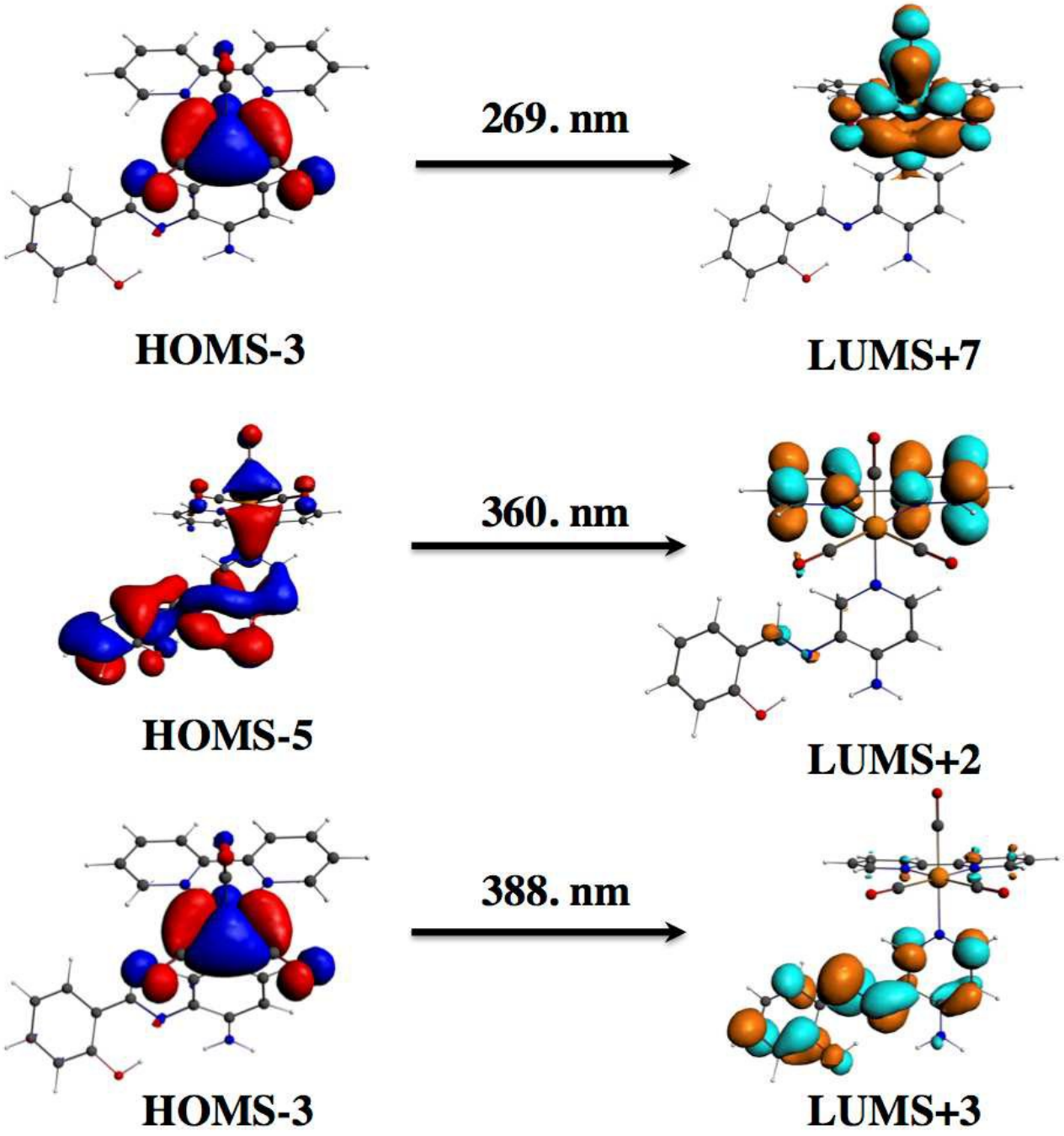

Figure 2. Assignment of the most important electronic transition for **C4**.

Figure 3 shows the room-temperature UV-vis absorption and emission spectra for **C3** and **C4** in acetonitrile (CH_3CN). **C3** shows a broad emission band, with a maximum at 610 nm, when the complex is excited at 445 nm. Under the same conditions of excitation for **C4**, a less intense broad emission band at 560 nm. These emission process are characteristic of Rhenium(I) tricarbonyl complexes and agree with the long lived MLCT excited states. [69] for Rhenium(I) tricarbonyl diimine compounds. A critical difference between compounds **C3** and **C4** is that they contain a redox active phenol group that is known to quench Rhenium(I) tricarbonyl compound excited states. [70] Therefore, we have ascribed the fast photoluminescent lifetimes to intramolecular electron transfer quenching of the ^{3}MLCT excited state by the phenolic functional group on the ligand coupled to proton transfer from the phenol to the nitrogen in the **L** ancillary ligand. This intramolecular quenching has been observed through flash quench experiments of a Ruthenium bipyridine compound. [71] The proton coupled electron transfer has also been observed for Rhenium(I) tricarbonyl compounds in intermolecular interactions. In support of this assignment we have found that the PL intensity is 2-3 times higher in 1.2 M D_2O/CH_3CN than in 1.2 M H_2O/CH_3CN (data not shown). Table 2 resume photophysical properties of **C3** and **C4**.

Table 2. Photophysical properties of *fac*-Re(CO)$_3$(**bpy**)**L(PF$_6$)** (**C3**) and *fac*-Re(CO)$_3$(**dmb**)**L(PF$_6$)** (**C4**) .

Compound	T (ns)	QY	k_r (M^{-1} s^{-1})	k_{nr} (M^{-1} s^{-1})
C3	< 10 [a]	< 0.001 [b]	10. x 10^{4} [c]	1.0 x 10^{8} [d]
C4	< 10 [a]	< 0.001 [b]	10. x 10^{4} [c]	1.0 x 10^{8} [d]

[a]Lifetimes were faster than the instrument response. [b]Within error quantum yields are zero. [c,d]These values are approximated.

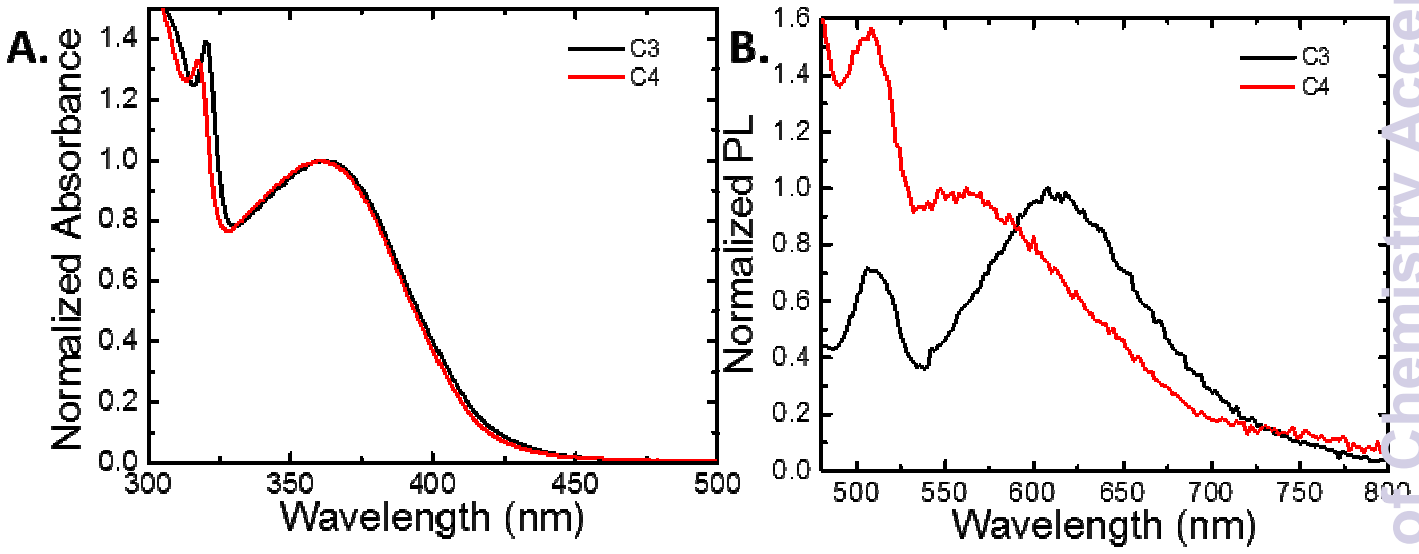

Figure 3. A) UV-Vis absorption and B) normalized photoluminescence spectra of *fac*-Re(CO)$_3$(**bpy**)**L(PF$_6$)** (**C3**) and *fac*-Re(CO)$_3$(**dmb**)**L(PF$_6$)** (**C4**) in CH_3CN.

The fluorescence spectra of **C3** and **C4** complexes, shows that the large Stokes shifts (λ_{ex}= 366 nm; λ_{em}= 610 nm for **C3** and λ ex= 361 nm; λ em= 560 nm for **C4**) can be observed, which also evidence a large changes in the dipole moment between the ground and excited states. On the other hand, **C3** and **C4** are very weak emitters with lifetimes less than 10 ns. The free (*E*)-2((3-amino-pyridin-4-ylimino)-methyl)-4,6-diterbutylphenol (**L**) ligand does not exhibit luminescence properties. This was described earlier by Carreño *et al*. [37-39]

3.2 Electrochemical studies.

The studies of cyclic voltammetry profiles showed several signals, which were solved by studying the working window potential. By comparing the stable profile of *fac*-Re(CO)$_3$(**bpy**)**Br** (**C1**), *fac*-Re(CO)$_3$(**dmb**)**Br** (**C2**), *fac*-Re(CO)$_3$(**bpy**)**L(PF$_6$)** (**C3**) and *fac*-Re(CO)$_3$(**dmb**)**L(PF$_6$)** (**C4**) compounds, Figure 4, several characteristics can be noticed.

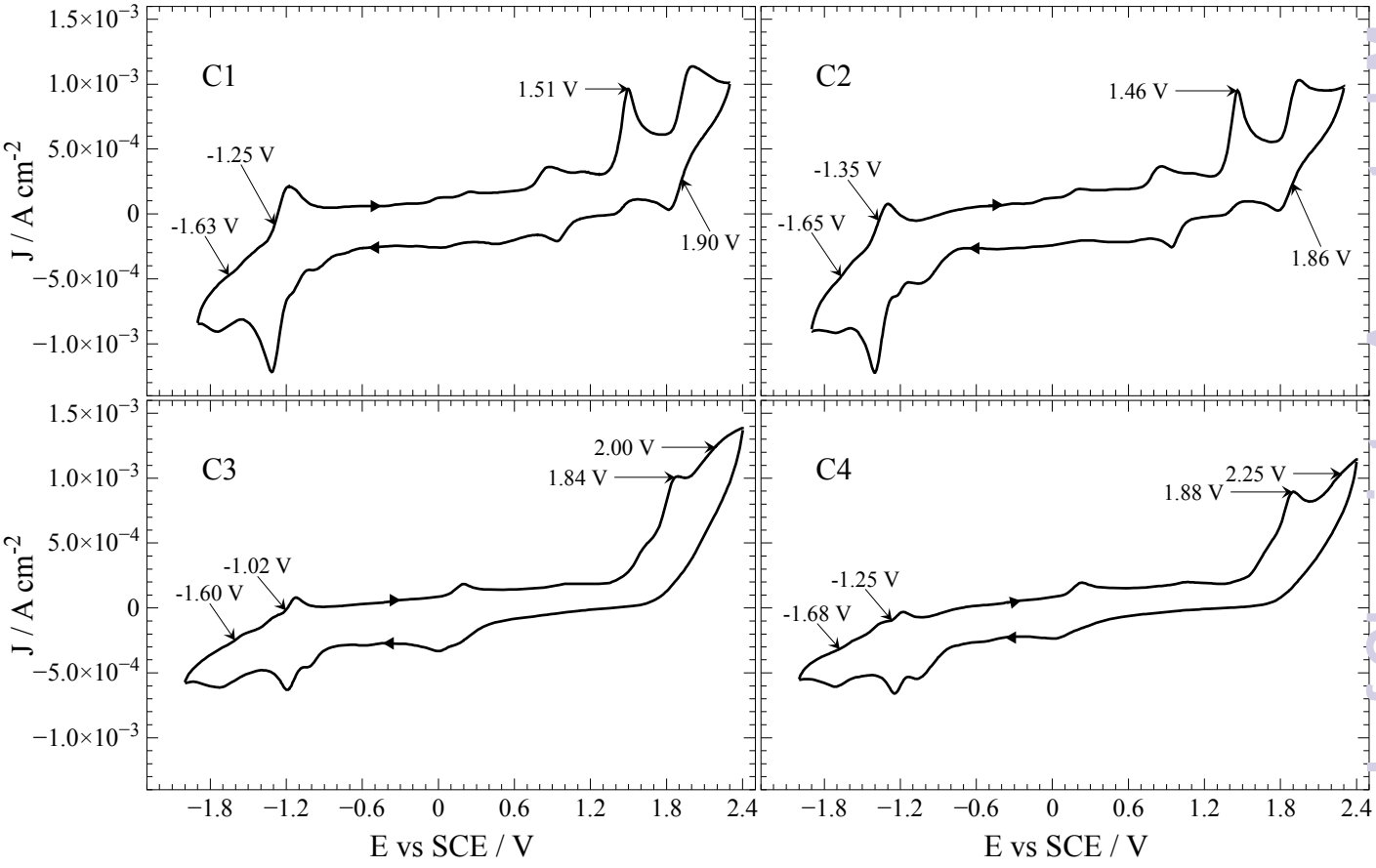

Figure 4. CV profiles of complexes. Interphase: Pt|1.0 x 10^{-2} M of compound + 1.0 x 10^{-1} M $TBAPF_6$ in anhydrous CH_3CN. Scan rate: 0.2 V s^{-1}.

In **C1**, rhenium oxidations appear at E_p 1.51 V, which seems to be electrochemically irreversible, and a second of reversible character at $E_{½}$ 1.90 V. On the other hand **C2** presents same peaks at E_p 1.46 V and $E_{½}$ 1.86 V, respectively. These results present similar values than those published by different authors using analogous complexes. [72-81] The first one-electron oxidation is electrochemically irreversible (i), probably by the repulsion of the positively charged species and the electrode (also positive during oxidation). Then follows the substitution of the halogen radical by rapid coordination of solvent generating *fac*-$Re^{I}(N,N)(CO)_3(ACN)^{-}$ (ii) (where N,N is **bpy** or **dmb** and ACN is acetonitrile). Finally, the second oxidation takes place (iii). The complete oxidation processes follows an electrochemical-chemical-electrochemical steps mechanism (ECE) (Czerwieniec *et al*. [72]), Scheme 2:

$$[Re^{I}(N,N)(CO)_3Br] \rightarrow [Re^{II}(N,N)(CO)_3Br]^{+} + e \quad \text{(i)}$$

$$[Re^{II}(N,N)(CO)_3Br]^{+} + ACN \rightarrow [Re^{I}(N,N)(CO)_3(ACN)]^{-} + Br^{-} \quad \text{(ii)}$$

$$[Re^{I}(N,N)(CO)_3(ACN)]^{\cdot} \leftrightarrows [Re^{II}(N,N)(CO)_3(ACN)]^{2+} + e \quad \text{(iii)}$$

N,N = **bpy** or **dmb**

ACN= Acetonitrile

Scheme 2. Reaction mechanism for **C1** and **C2** reversible oxidations.

In addition, according to the cyclic voltammetry study, there are two reversible reduction processes (more distinguishable at the working window study, see Figures S16-S19 in the ESI†). For **C1** at $E_{½}$ -1.25 V and -1.63 V. For **C2** at $E_{½}$ -1.35 V and -1.65 V instead. The firsts less negative processes may be attributed to the reversible reduction of the bipyridine-based ligands N,N (where N,N is **bpy** or **dmb**) (iv). The seconds more negative correspond to the Re^{I}/Re^{0} reduction [37] (vi). Regardless if these reductions processes may be attributed specifically to a particular moiety, by the shape and position of the peaks its seems that the electrochemical reduction processes also follows a typical electrochemical-eletrochemical-chemical mechanism (EEC) (Manbeck *et al.* [73]) with bromide dissociation as the chemical step (v and vii), Scheme 3:

$$[Re^{I}(N,N)(CO)_3Br] + e \leftrightarrows [Re^{I}(N,N)(CO)_3Br]^{-} \quad (iv)$$

$$[Re^{I}(N,N)(CO)_3Br]^{-} \rightarrow [Re^{I}(N,N)(CO)_3] + Br^{-} \quad (v)$$

$$[Re^{I}(N,N)(CO)_3Br]^{-} + e \leftrightarrows [Re^{0}(N,N)(CO)_3Br]^{2-} \quad (vi)$$

$$[Re^{0}(N,N)(CO)_3Br]^{2-} \rightarrow [Re^{0}(N,N)(CO)_3]^{-} + Br^{-} \quad (vii)$$

N,N = **bpy** or **dmb**

Scheme 3. Reaction mechanism for **C1** and **C2** reversible reductions.

The kinetic description for **L**-containing complexes (**L** is (E)-2((3-amino-pyridin-4-ylimino)-methyl)-4,6-diterbutylphenol ancillary ligand) is quite similar, without the bromide elimination steps. Reduction processes may be assigned to be of the same nature than those described for **C1** and **C2**. Regarding the oxidations, both **L**-containing complexes had two irreversible ones, the first at 1.84 and 1.88 V and the seconds more energetics at 2.00 and 2.25 V for **C3** and **C4**, respectively (all defined, see Figures S18-S19 in the ESI). Judging by their shape and positions the mechanism corresponds to an ECE one as well as it was described for analogous alkynyl complexes. After Re^{I}/Re^{II} oxidation (viii), it follows a chemical step consisting on an intramolecular redox reaction between the rhenium center Re^{II}/Re^{I} (reduction) and (*E*)-2((3-amino-pyridin-4-ylimino)-methyl)-4,6-diterbutylphenol (**L**) ancillary ligand (oxidation), with the instant substitution of radical $\mathbf{L}^{-}$ specie by a solvent molecule (ix). As a final step, a second oxidation of the Re^{I}/Re^{II} center takes place (x) as described by the following mechanism (Lam et al. [74]), Scheme 4:

$$[Re^{I}(N,N)(CO)_3L] \rightarrow [Re^{II}(N,N)(CO)_3L]^{+} + e \quad (viii)$$

$$[Re^{II}(N,N)(CO)_3L]^{+} + ACN \rightarrow [Re^{I}(N,N)(CO)_3(ACN)]^{-} + L^{-} \quad (ix)$$

$$[Re^{I}(N,N)(CO)_3(ACN)]^{-} \rightarrow [Re^{II}(N,N)(CO)_3(ACN)]^{2+} + e \quad (x)$$

N,N = **bpy** or **dmb**

L= (*E*)-2((3-amino-pyridin-4-ylimino)-methyl)-4,6-diterbutylphenol

ACN= acetonitrile

Scheme 4. Reaction mechanism for **C3** and **C4** irreversible oxidations.

The elimination of the (*E*)-2((3-amino-pyridin-4-ylimino)-methyl)-4,6-diterbutylphenol (**L**) explains the irreversible character of these oxidations for **C3** and **C4**; if as a consequence of an electrochemical process an important structural change takes place on the analyte, such process would be surely irreversible in nature. For the ligand **L** it has been reported [38] only two irreversible oxidation processes of much less intensity (E_p 0.71 and1.35 V vs SCE); these were not observed in **C3** and **C4**, probably due the high intensity of the Rhenium oxidation peaks. Nevertheless, the replacement of Br^- by **L** has a notorious influence on the oxidation value for $Re^I \rightarrow Re^{II}$. Peak description is summarized on Table 3.

Table 3. CV-profile peak description for the electrochemical processes for **C1**, **C2**, **C3** and **C4** complexes (in acetonitrile).

Process	E^I_{ox} (V)	E^{II}_{ox} (V)	E^I_{red} (V)	E^{II}_{red} (V)
Assignment	$Re^I \rightarrow Re^{II}$		N,N reduction	$Re^I \rightarrow Re^0$ [78-81]
C1	1.51_i	1.90_r	-1.25_r	-1.63_r
C2	1.46_i	1.86_r	-1.35_r	-1.65_r
C3	1.84_i	2.00_i	-1.02_r	-1.60_r
C4	1.88_i	2.25_i	-1.25_r	-1.68_r

i, irreversible

r, quasi- or fully-reversible

In this sense, $Re^I \rightarrow Re^{II}$ oxidation occurs at higher potentials in **L**-containing complexes (**C3** and **C4)** relative to the precursor (**C1** and **C2**), which means that (*E*)-2((3-amino-pyridin-4-ylimino)-methyl)-4,6-diterbutylphenol (**L**) has an electron-withdrawing effect over the positive charge on the rhenium atom, explaining the value shift. The change on the reversible character at E^{II}_{ox} process is instead explained by the above-mentioned mechanism [74], Scheme 4.

On the other hand, the electron-withdrawing effect of (*E*)-2((3-amino-pyridin-4-ylimino)-methyl)-4,6-diterbutylphenol (**L**) provoke that reduction processes require less energy to occur. For instance, **bpy** or **dmb** reduction (E^{I}_{red}) in **C3** and **C4**, respectively, takes places at a less negative potential compared to their precursors **C1** and **C2**. Such behavior may also be explained by the fact that **C3** and **C4** has no halide attached to its core; since no chemical dissociation step occurs during the mechanism; then, by preventing bromide (strong anionic character) liberation in anhydrous solvent, the required potential for reduction of **C3** and **C4** decreases (requires less energy). Such electron-withdrawing character of **L** was reported on previous studies with analogous complexes using different bypiridine ligand: 4,4'-$(ethanoate)_2$-2,2'-bipyridine (**deeb)** [37]. That study showed that when passing complex transformation from $Re(CO)_5Br$, $[Re(CO)_3(\mathbf{deeb})Br]$ to $[Re(CO)_3(\mathbf{deeb})\mathbf{L}]^+$ metallic center reduction $Re^{I} \rightarrow Re^{0}$ shifted from -1.74, -1.25 and -1.18 V. Also **deeb** reduction potential shifted to less negative values after **L** addition; [37] practically the same was observed on the present study. Hence, the nature of **L** and its effect on rhenium complexes electrochemical features is once more corroborated: the electron-withdrawing character of **L** ancillary ligand has an effect, going through the metallic center and affecting the bipyridine-based ligands redox-processes.

3.3 Cytotoxicity essays for C3 and C4 complexes

To infer that the *fac*-Re(CO)$_3$(**bpy**)**L**(PF$_6$) (**C3**) and *fac*-Re(CO)$_3$(**dmb**)**L**(PF$_6$) (**C4**), see Scheme 1, induced cytotoxicity, we performed a modification of the neutral red uptake assay. [51-52] Epithelial cells (T84) were co-incubated 24 h with different concentrations of either **C3** or **C4** prior to performing the neutral red uptake assay. As shown in Figure 5, 12.50 ppm (in 3.13% DMSO) of each compound was sufficient to decrease the cell viability in almost 90%. By contrast, 3.13% DMSO alone (control) only decreases cell viability in approximately 50%. Higher or lower concentrations were indistinguishable from the vehicle (DMSO) alone. Interestingly, with 200 ppm it was possible to observe an apparent higher viability. This effect might be due to cell fixation because of the high concentration of DMSO, as assessed by optical microscopy (data not shown). From these data, we decided to perform cell staining with **C3** and **C4** using 200 ppm diluted in one part of DMSO and in one part of an aqueous solution.

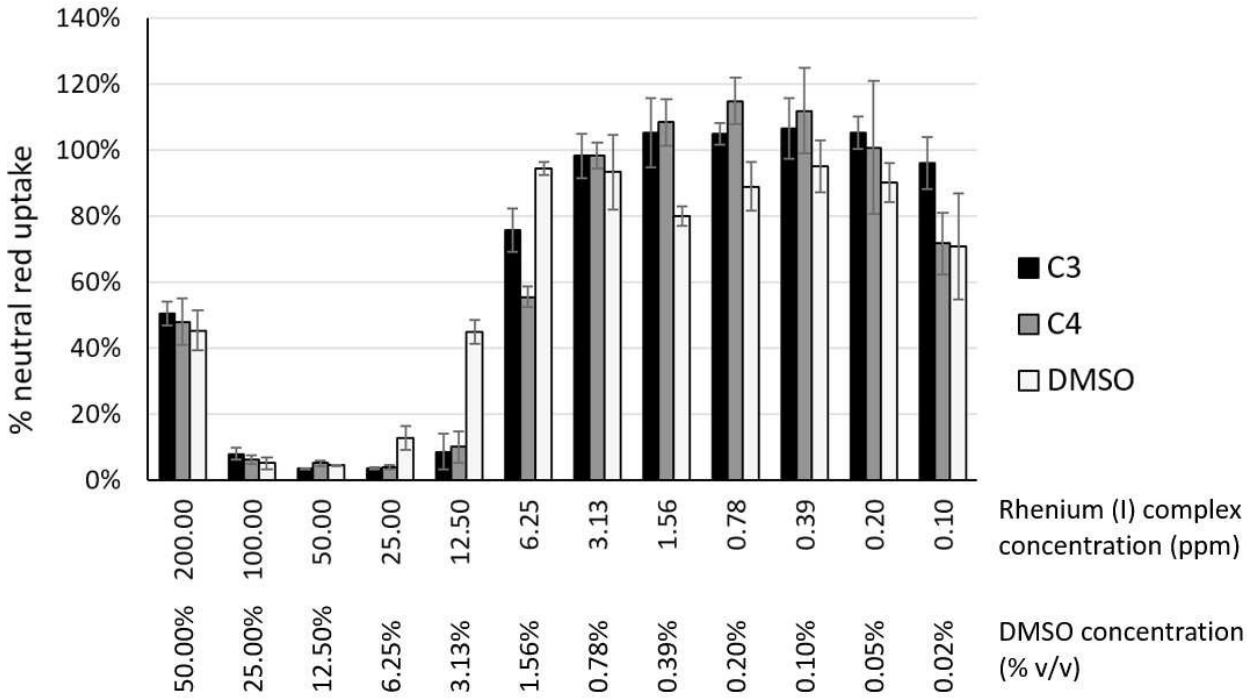

Figure 5. Determination of the cytotoxicity induced by either **C3** (black) or **C4** (gray) in an epithelial cell line (T84), inferred by the neutral red uptake assay. The 100% of neutral red uptake was determined from untreated cells. As control, DMSO (light gray) alone was diluted in the same way than the Re (I) complexes to discard the cytotoxicity effect produced by the vehicle. The DMSO concentration (% v/v) depicted in the figure is valid for **C3**, **C4** and for the control (DMSO alone). This experiment was performed in triplicate.

3.4 Cell staining

In order to study the suitability of the *fac*-Re(CO)$_3$(**bpy**)**L(**PF$_6$**)** (**C3)** and *fac*-Re(CO)$_3$(**dmb**)**L(**PF$_6$**)** (**C4)** compounds as fluorophores for cellular imaging, we performed fluorescent microscopy assays [64-66]. **C3** and **C4** Rhenium(I) tricarbonyl complexes (see Scheme 1) were used for preliminary cell microscopy studies on bacteria. For that, cultured *Salmonella enterica* serovar Typhimurium (*S. enterica*, a Gram-negative bacterium) was cultured in LB broth to stationary phase (OD_{600} = 1.4), washed with PBS and treated with either **C3** or **C4** (final concentration: 200 ppm, see details in Materials and Methods) for only 5 min at 37 °C. Stained bacteria were washed three times with PBS and fresh samples were observed under confocal microscopy with an objective of 100X. DMSO alone, instead of **C3** or **C4,** was used to set the detection threshold. As shown in Figure 6, both **C3** and **C4** can be efficiently used to reveal *S. enterica* through confocal microscopy, demonstrating that these Rhenium(I) tricarbonyl complexes can be used as rapid and stable fluorescent dyes for bacteria. As next step, we assessed whether **C3** and **C4** were suitable to stain eukaryotic cells, including yeasts (*Candida albicans* and *Cryptococcus* spp.) and human cells (SKOV-3 and HEK-293). Yeasts were mixed with the Rhenium(I) tricarbonyl complexes and treated as described for bacteria. As previously reported, yeasts exhibit autofluorescence, emitting in the range of UV. [82] Autofluorescence, apparently produced by components found in the fungal wall as inferred by figures 7 and 8, was useful to identify the position of the fungal cells without the need of other fluorophores to that end. As observed in Figures 7 and 8, it was possible to stain yeasts with either **C3** or **C4**. Interestingly, **C3** or **C4** seemed to differentially stain buds or newer, smaller cells (Figure 6), while **C3** tended to be retained in cells presenting thinner cell walls (Figure 7). These results suggest that these Rhenium(I) tricarbonyl compounds could be used to discriminate distinct cell types (see Figure S20 in the ESI†). Nevertheless, more experiments are needed to test this hypothesis.[83-87]

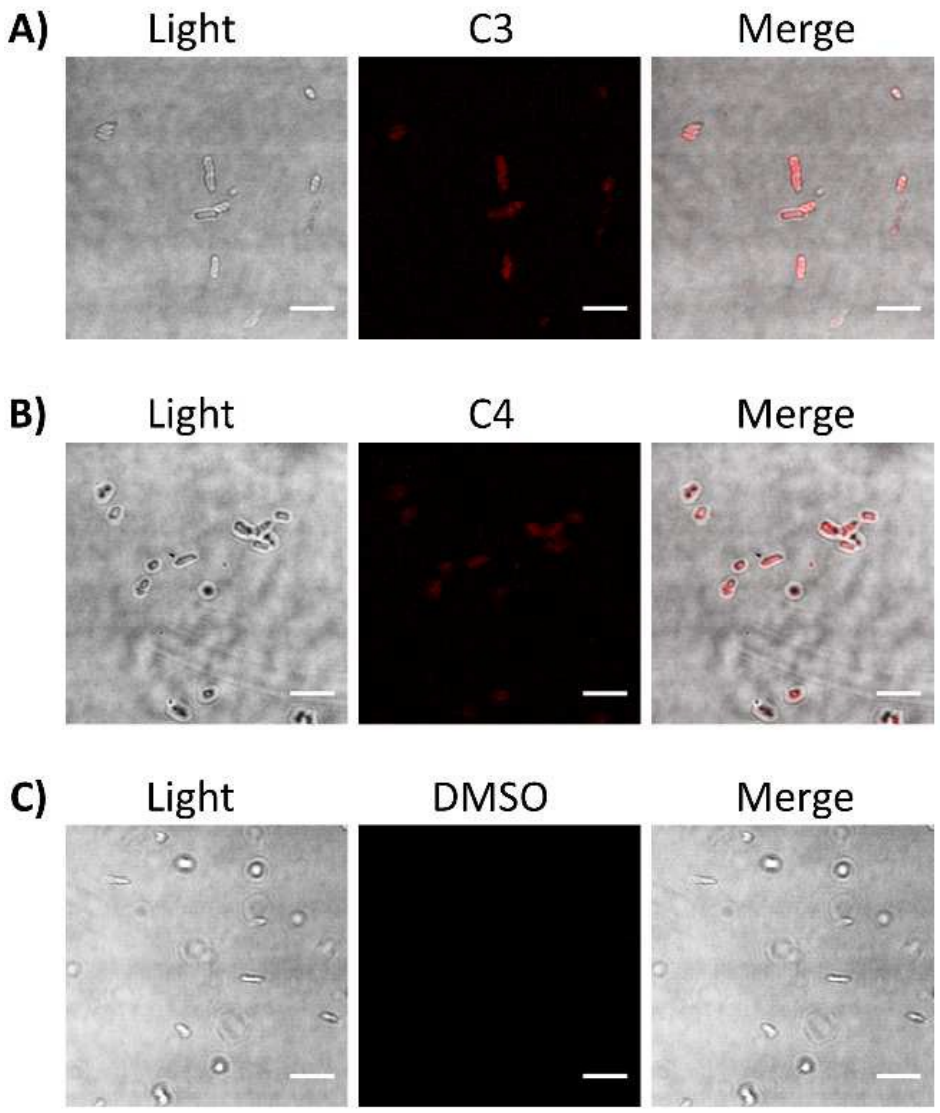

Figure 6. Fluorescence confocal microscopy images showing bacteria (*Salmonella enterica*) stained with either **C3** (A) or **C4** (B). DMSO alone was used to set the detection threshold (C). In all the cases, the microorganisms were observed fresh, using a 100X objective. White bars represent 5 µm.

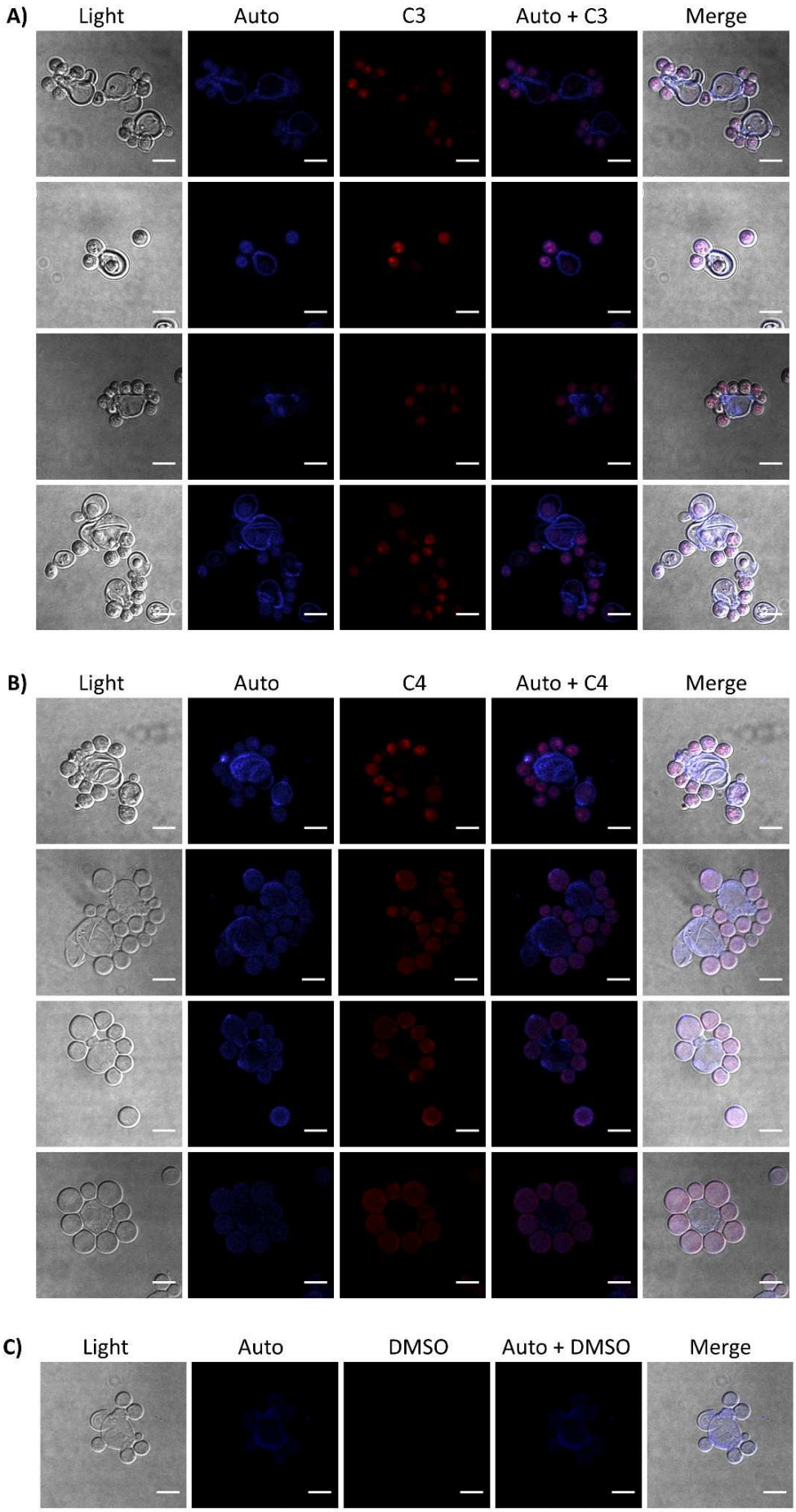

Figure 7. Fluorescence confocal microscopy images showing *Candida albicans* (yeast) stained with either **C3** (A) or **C4** (B). DMSO alone was used to set the detection threshold (C). In all the cases, the microorganisms were observed fresh, using a 100X objective. White bars represent 5 µm.

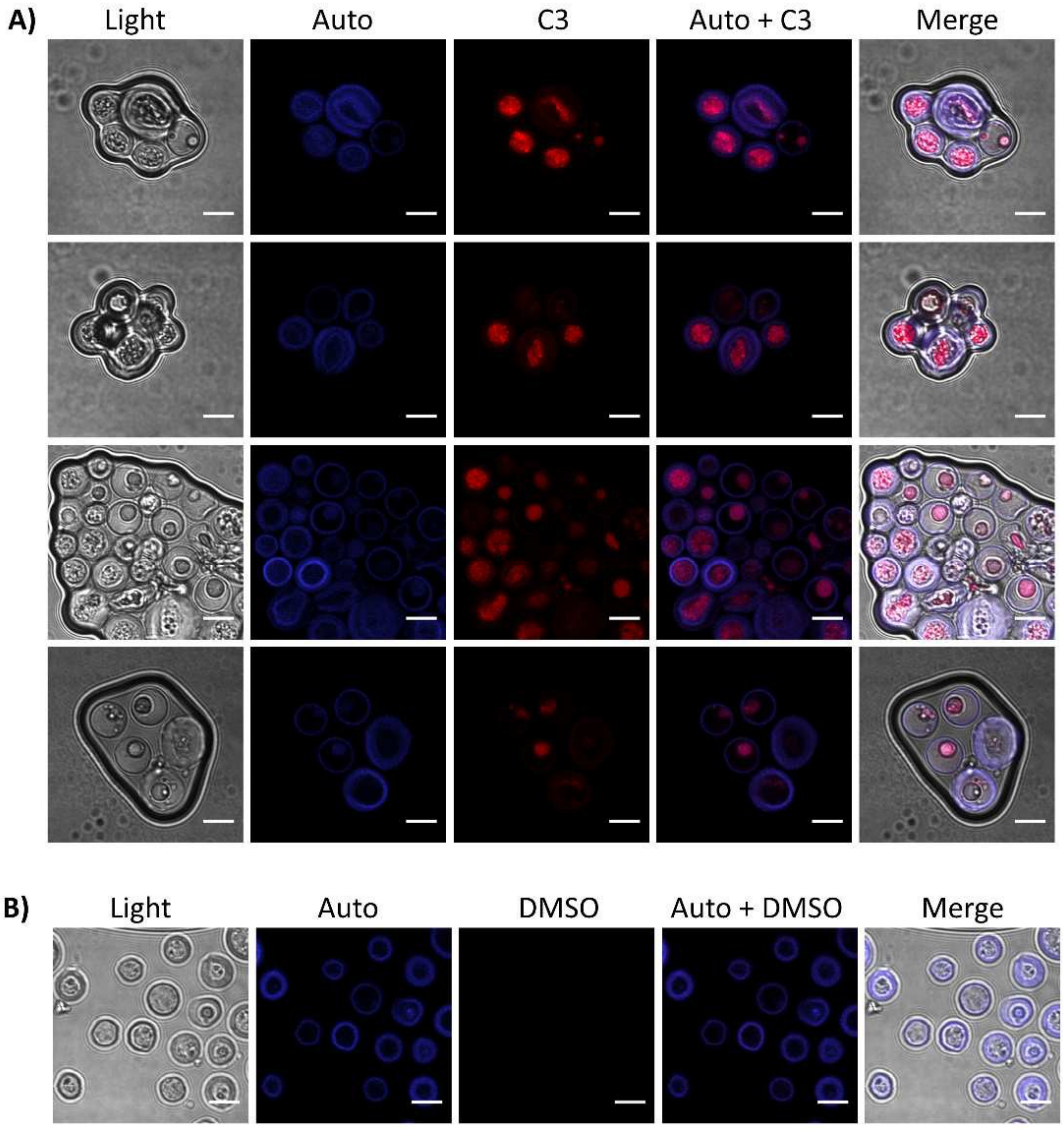

Figure 8. Fluorescence confocal microscopy images showing *Cryptococcus* spp. (yeast) stained with either **C3** (A). **C4** was also able to stain *Cryptococcus* spp. (see Figure S20 in the Supplementary material). DMSO alone was used to set the detection threshold (B). In all the cases, the microorganisms were observed fresh, using a 100X objective. White bars represent 5 µm.

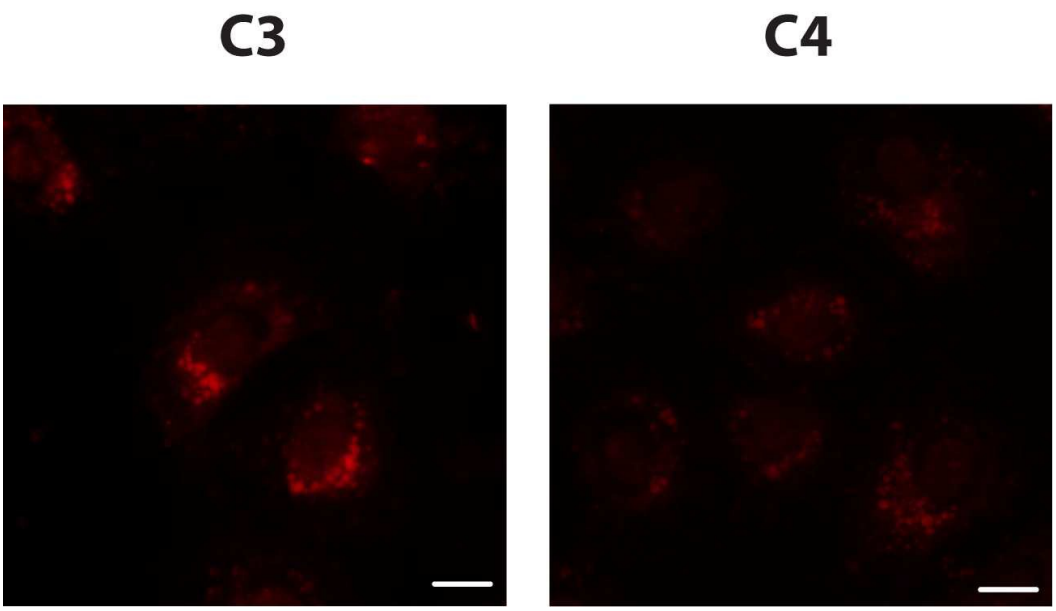

Figure 9. Fluorescence microscopy images showing SKOV3 cells fixed after treatment with **C3** or **C4** 44 ppm for 48 h. White bars represent 10 μm.

To determine whether *fac*-Re(CO)$_3$(**dmb**)**L(**PF$_6$**)** (**C3)** and *fac*-Re(CO)$_3$(**dmb**)**L(**PF$_6$**)** (**C4)** can also be used to stain human cells, we tested a human ovarian cancer cell line (SKOV-3) [88-94]. Incubation of our complexes was carried out on adherent cells, which were seeded on 24-well plates at 24 and 48 h prior to the experiment. Our results showed the suitability of the described Re (I) complexes for cell microscopy applications. Fluorescent images (Figure 9) clearly showed a punctuate distribution of exogenous Rhenium(I) tricarbonyl complexes. [95-97] During our microscopic investigations, we did not observe any photobleaching effects or loss of fluorescence intensity, which are well known for most organic dyes, especially during extended exposure times. [98-103]

In general, both tested compounds were able to stain cells showing a punctuated distribution in the cytoplasm, whereas nuclear membrane seems to be impermeable to our compounds, (shown in Figure 10) by no colocalization with a specific nuclear label (Hoescht dye). [103] Distribution of the compounds is similar in an embryonic kidney cell line (HEK-293) and in primary cell culture derived from human placenta showing no difference between a cancer cell and a healthy one (data not shown).

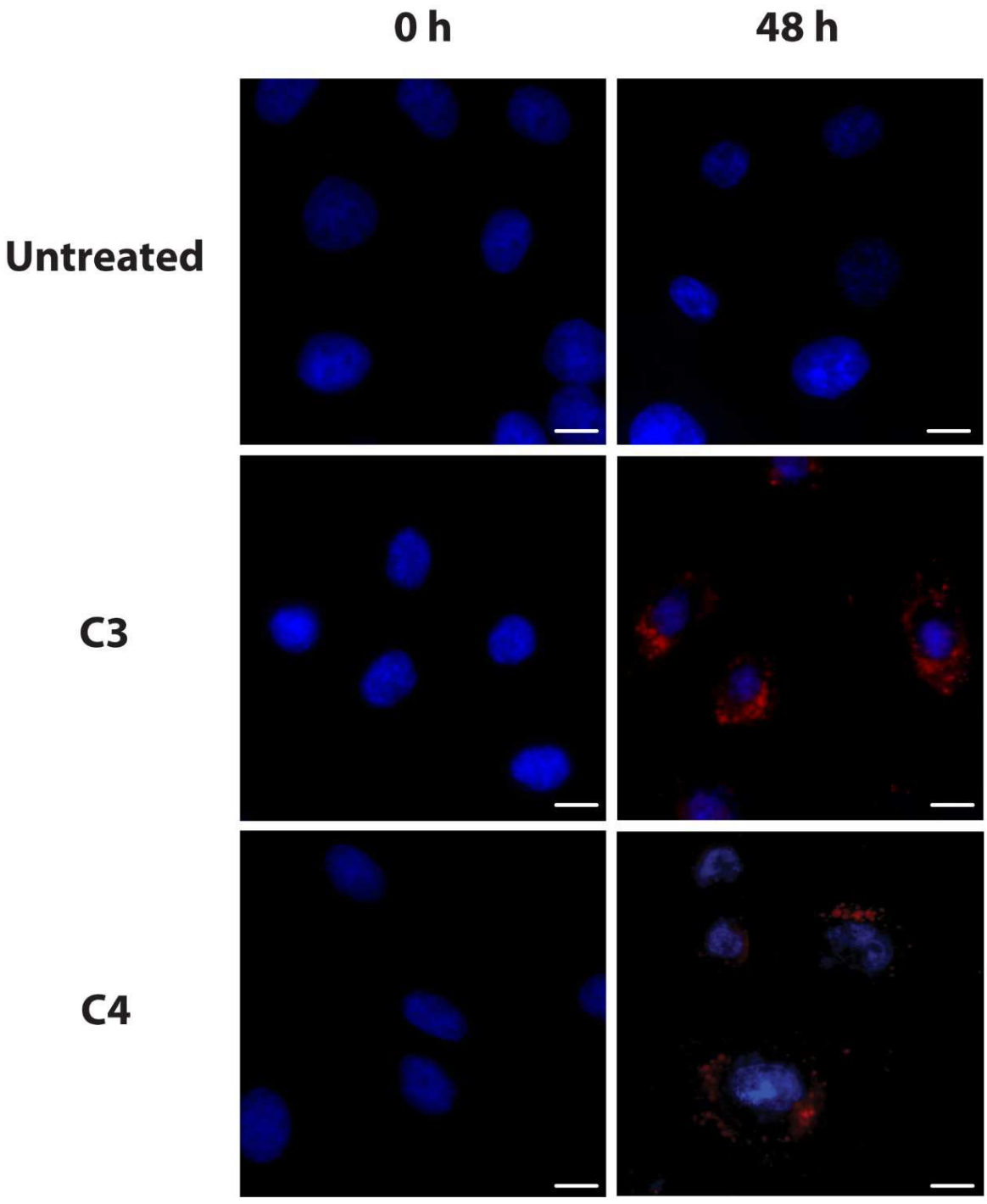

Figure 10. Fluorescence microscopy images showing SKOV-3 cells fixed after treatment with **C3** or **C4** 44 ppm for 48 h. Hoechst was used to label nuclear DNA. White bars represent 5 μm.

4. Conclusions

In the present work, we have reported the synthesis of a new kind of Rhenium(I) tricarbonyl complexes containing the *fac*-$Re(CO)_3$(**dmb**)$^+$ core and the ancillary ligand Schiff base (E)-2-((3-amino-pyridin-4-ylimino)-methyl)-4,6-diterbutylphenol (**L**), harboring an intramolecular hydrogen bond, as ancillary ligand. [104] In particular, we reported *fac*-$Re(CO)_3$(**bpy**)**L(**PF_6**)** (**C3**) and *fac*-$Re(CO)_3$(**dmb**)**L(**PF_6**)** (**C4**), where **bpy** is a 2,2'-bipyridine and **dmb** is 4,4'-dimethyl-2,2'-bipyridine. This work is framed in the development of new Rhenium(I) tricarbonyl complexes with alternative ancillary ligands aimed to obtain improved biomarkers by modulating their physicochemical properties. In order to modulate the photophysical properties of Rhenium(I) tricarbonyl core, most research has been focused in the bidentate ligand substituting the corresponding aromatic rings with different donor or acceptor groups. [105-107] On the other hand, the ancillary (i.e. "secondary") ligand has been commonly, ignored; only the use of halogens at this position has been described. Accordingly, it has been postulated that the bidentate ligand is one of the most important modifier of the Rhenium (I) tricarbonyl properties. By contrast, we have seen that the ancillary ligand, depending on its nature, may be an important modulatory agent, modifying the physicochemical properties of the Rhenium (I) tricarbonyl core [108-111], including luminescence (quantum yields, lifetime, Stokes shift), electrochemical properties and biocompatibility, as it has been also supported by a previous work. [37-39] In particular, we have observed that new potential ancillary ligands (i.e. (*E*)-2-((3-amino-pyridin-4-ylimino)-methyl)-4,6-diterbutylphenol (**L**)) affect some of the electronic properties of the Rhenium(I) tricarbonyl complexes. [37]

From the chemical point of view, the most interesting properties found in **C3** and **C4**, including the fluorescence and the electrochemical profile, can be attributed to the nature of the. (*E*)-2-((3-amino-pyridin-4-ylimino)-methyl)-4,6-diterbutylphenol (**L**) ancillary ligand and the intramolecular nature of this PCET reaction [112-114] observed in **C3** and **C4** complexes is of high interest and will be more thoroughly investigated in future works. The electron-withdrawing nature of the **L** ancillary ligands in **C3** and **C4** complexes were observed by ^{1}H-NMR, absorption and electrochemical studies. Also, a correlation between the electron withdrawing effect from the ligand **L** and the redox potential values were also observed. Oxidation peaks positions shifts when switching from precursors **C1** and **C2** to complexes **C3** and **C4**, revealing the assumed electron-withdrawing effect of the **L** ancillary ligand in the Rhenium (I) tricarbonyl complexes and its importance in the modulation of the Re (I) tricarbonyl

properties. In **C3**, rhenium oxidation appears at 1.84 V and at 1.88 V for **C4,** also confirming this effect.

Respect to the properties of the structure of the ancillary ligands **L** and their tert-butyl donor groups, the electron withdrawing effect may be probably related to the presence of the intramolecular hydrogen bond and was confirmed by theoretical calculations. The electronic transitions of **C4** computed by a TDDFT method including SO relativistic effects show good agreement with the experimental data. The electronic studies showed that the absorption band is dominated by MLCT (HOMS-3→LUMS+2) and LLCT (HOMS-5→LUMS+2) transition at 360 nm for **C4** which involve orbitals located in the hydrogen bond of the ancillary ligand (**L**).

Live-cell fluorescence microscopy of the new compounds **C3** and **C4** confirmed their potential as fluorescent dyes for both prokaryotic and eukaryotic cells (including fungal and mammalian cells). **C3** and **C4** can be used to perform a rapid staining of bacteria (*Salmonella enterica*) and yeasts (*Candida albicans* and *Cryptococcus* spp.) in only 5 min, remarking their properties to interact with microorganisms in short periods. Furthermore, the Rhenium (I) tricarbonyl complexes **C3** and **C4** apparently accumulate differentially in fungal cells, underlining a potential use as fluorescent differential dyes with no need of combination with antibodies. [115]

Finally, both **C3** and **C4** complexes were captured by SKOV-3 and HEK-293 cells, revealing discrete structures, suggesting that these compounds present affinity for specific zones or organelles inside the cell. In summary, in this work we reported two new Rhenium(I) tricarbonyl complexes with an electron withdrawing ancillary ligand (**L**), showing suitable properties to be used as novel fluorescent dyes for biological purposes.

Supporting Information: Supplementary data associated with this article can be found, in the online version.

Acknowledgements

Funded by Project RC120001 of the Iniciativa Científica Milenio (**ICM**) del Ministerio de Economía, Fomento y Turismo del Gobierno de Chile, FONDECYT 1150629 and Proyecto Núcleo UNAB DI-1419-16/N; E. Molins acknowledges funding by the Spanish Ministerio de Economía y Competividad (ENE2015-63969 and SEV2015-0496). The authors acknowledges The UNC Department of Chemistry Mass Spectrometry Core Laboratory for the acquisition of mass spectra. We are grateful to Dr. Maria A. Del Valle (UC) and Luis Velasquez (CIMIS) for instrumentals facilities. Thanks to Dr. Andres Vega (UNAB) for valuable discussion and B.A. Alfonso Inzunza G. for his help with the English translation.

References

[1] B.L. Haas; J.S. Matson; V.J. DiRita; J.S. Biteen; *Molecules*, 2014, **19** , 12116

[2] K.L. Haas; K.J. Franz; *Chemical reviews*, 2009, **109** , 4921

[3] B.N. Giepmans; S.R. Adams; M.H. Ellisman; R.Y. Tsien; *Science*, 2006, **312** , 217

[4] M. Baker; *Nat Methods,* 2010, **7**, 957

[5] T.L. Doane; C. Burda; *Chemical Society reviews*, 2012, **41**, 2885

[6] L. Shang; S.J. Dong; G.U. Nienhaus; *Nano Today*, 2011, **6** , 401

[7] G.S. Baird; D.A. Zacharias; R.Y. Tsien; *Proceedings of the National Academy of Sciences of the United States of America*, 2000, **97**, 11984

[8] N.C. Shaner; R.E. Campbell; P.A. Steinbach; B.N. Giepmans; A.E. Palmer; R.Y. Tsien; *Nature biotechnology*, 2004, **22**, 1567

[9] M. Patra; G. Gasser; *European journal of chemical biology*, 2012,**13**, 1232

[10] M.P. Coogan; V. Fernandez-Moreira; 2014. *Chem Commun (Camb)*, 2014, **50**, 384

[11] V. Sathish; E. Babu; A. Ramdass; Z.Z. Lu; M. Velayudham; P. Thanasekaran; K.L. Lu; S. Rajagopal; *Talanta*, 2014, **130**, 274

[12] M. Wrighton, D. Morse, *J. Am. Chem. Soc*., 1979, **101**, 2888.

[13] R. Alberto, R. Schibli, A. Egli, P.A. Schubiger, *J. Am. Chem. Soc*., 1998, **120**, 7987

[14] R. Schibli, A.P. Schubiger, *Eur. J. Nucl. Med.* 2002, **29**, 1299

[15] T. M. McLean, J. L. Moody, M. R. Waterland, S. G. Telfer, *Inorg. Chem*, 2012, **51**, 446

[16] E. E. Langdon-Jones, N. O. Symonds, S. E. Yates, A. J. Hayes, D. Lloyd, R. Williams, S. J. Coles, P. N. Horton, S. J.A. Pope, *Inorg. Chem,* 2014, **53**, 3788

[17] D.K. Orsa, G.K. Haynes, S.K. Pramanik, M.O. Iwunze, G.E. Greco, D.M. Ho, J.A. Krause, D.A. Hill, R. J. Williams, S.K. Mandal, *Inorg. Chem. Comm*., 2008, **11**, 1054.

[18] A. El Nahhas , A. Cannizzo, F. van Mourik, A.M. Blanco-Rodriguez, S. Zalis, A. Vlcek, M. Chergui, *J. Phys. Chem. A,* 2010, **114**, 6361.

[19] T.M. McLean, J.L. Moody, M.R. Waterland, S.G. Telfer, *Inorg. Chem*., 2012, **51**, 446.

[20] L.A. Worl, R. Duesing, P. Chen, L. Della Ciana, T.J. Meyer, *J. Chem. Soc. Dalton Trans*. 1991, 849.

[21] G.M. Hasselmann, G.T. Meyer, *J. Phys. Chem. B*, 1999, **103**, 7671.

[22] R. Alberto, R. Schibli, R. Waibel, U. Abram, A.P. Schubiger, *Coord. Chem. Rev*., **190** (1999) 901.

[23] A. Leonidova, G. Gasser, *ACS Chem. Biol*., 2014, **9** , 2180

[24] S. James, K. P. Maresca, J. W. Babich, J. F. Valliant, L. Doering, J. Zubieta, *Bioconjugate Chem*., 2006, **17**, 590

[25] F. L. Thorp-Greenwood, *Organometallics*, 2012, **31**, 5686

[26] S. W. Botchway, M. Charnley, J. W. Haycock, A. W. Parker, D. L. Rochester, J. A. Weinstein, J. A. Gareth Williams, PNAS, 2008, **42**, 16071

[27] S. Faulkner, S. J. A. Pope, B. P. Burton-Pye, *Applied Spectroscopy Reviews*, 2005, **40**, 1

[28] A.J. Amoroso, M.P. Coogan, J.E. Dunne, V. Fernandez-Moreira, J.B. Hess, A.J. Hayes, D. Lloyd, C. Millet, S.J.A. Pope, C. Williams, Chem. Commun., 2007, 3066.

[29] A.J. Amoroso; R.J. Arthur; M.P. Coogan; J.B. Court; V. Fernandez-Moreira; A.J. Hayes; D. Lloyd; C. Millet; S.J.A. Pope; *New J. Chem*; 2008, **32**, 1097

[30] L.A. Worl; R. Duesing; P.Y. Chen; L. Dellaciana; T.J. Meyer; *J. Chem Soc Dalton*, 1991, 849

[31] L. Hammarstrom; S. Hammes-Schiffer; *Accounts of chemical research*, 2009, **42**, 1859

[32] Y. Terazono; G. Kodis; K. Bhushan; J. Zaks; C. Madden; A.L. Moore; T.A. Moore; G. R. Fleming; D. Gust; *J. Am. Chem. Soc.* 2011, **133**, 2916

[33] G.F. Moore; M. Hambourger; G. Kodis; W. Michl; D. Gust.; T.A. Moore; A.L. Moore; *J. Phys. Chem.* 2010, **114**,14450

[34] D. Gust; T.A. Moore; A.L. Moore; *Acc. Chem. Res.* 2009, **42**,1890

[35] A.W. Kleij, M. Kuil, D.M. Tooke, M. Lutz, A.L. Spek., J.N.H. Reek, *Chem. Eur. J*., 2005, **11**, 4743.

[36] A. Carreño, A. Vega, X. Zarate, E. Schott, M. Gacitua, N. Valenzuela, M. Preite, J.M. Manriquez, I. Chavez, *Quim. Nova*, 2014, **37**, 584

[37] A. Carreño, M. Gacitua, E. Schott, X. Zarate, J.M. Manriquez, M. Preite, S. Ladeira, A. Castel, N. Pizarro, A. Vega, I. Chavez, R. Arratia-Perez, *New J. Chem*, 2015, **39**, 5725

[38] A. Carreño; M. Gacitua; D. Paez-Hernandez; R. Polanco; M. Preite; J.A. Fuentes; G. Mora; I. Chavez; R. Arratia-Perez; New J. Chem, 2015, **39**, 7822

[39] A. Carreño; M. Gacitua; J.A. Fuentes; D. Paez-Hernandez; C. Araneda; I. Chavez; M. Soto-Arriaza; J.M. Manriquez; R. Polanco; G.C. Mora; C. Otero; W.B. Swords; R. Arratia-Perez, *New J. Chem.*, 2016, **40**, 2362

[40] L. Sacksteder, A.P. Zipp, E.A. Brown, J. Streich, J.N. Demas, B.A. DeGraff, *Inorg. Chem*., 1990, **29**, 4335.

[41] M. Y. Berezin, S. Achilefu, *Chem. Rev*., 2010, **110**, 2641

[42] L. Raszeja, A. Maghnouj, S. Hahn, N. Metzler-Nolte, *ChemBioChem*., 2011, **12**, 371

[43] M. K. Mbagu, D. N. Kebulu, A. Winstead, S. K. Pramanik, H. N. Banerjee, M. O. Iwunze, J. M. Wachira, G. E. Greco, G. K. Haynes, A. Sehmer, F. H. Sarkar, D. M. Ho, R. D. Pike, S. K. Mandal, *Inorganic Chemistry Communications*, 2012, **21**, 35

[44] G. B. Blakney, W. F. Allen, *Inorg. Chem.* 1971, **10**, 2763

[45] A. M. Bond, R. Colton, M. E. McDonald, *Inorg. Chem*, 1978, **17**, 2842

[46] R. Lopez, B. Loeb, D. Striplin, M. Devenney, K. Omberg, T. J. Meyer, *J. Chil. Chem. Soc*., 2004, **49**, 149

[47] A. M. Bond, R. Colton, M. E. McDonald, *Inorg. Chem*, 1978, **17**, 2842

[48] Amsterdam Density Functional (ADF) Code, Vrije Universiteit: Amsterdam, 2007.

[49] P. Pyykko, Chem. Rev., 1988, 88, 563

[50] L. Verluis and T. Ziegler, J. Chem. Phys., 1988, **88**, 322.

[51] D. Paez-Hernandez, J. Murillo-Lopez and R. Arratia-Perez, Organometallics, 2012, **31**, 6297.

[52] L.M. Valenzuela; A.A. Hidalgo; L. Rodríguez; I.M. Urrutia; A.P. Ortega; N.A. Villagra; D. Paredes-Sabja; I.L. Calderón; F. Gil; C.P. Saavedra; G.C. Mora; J.A. Fuentes; *Infect. Genet. Evol.* 2015, **33**, 131

[53] F.L. Thorp-Greenwood; M.P. Coogan; Dalton Trans, 2011, **40**, 6129

[54] E. Vergara; E. Cerrada; A. Casini; O. Zava; M. Laguna; P. J. Dyson; Organometallics, 2010, **29**, 2596

[55] F.L. Thorp-Greenwood; M.P. Coogan; L. Mishra; N. Kumari; G. Rai; S. Saripella; New J. Chem. 2012, **36**, 64

[56] L.E. Roy, T. Hughbanks, *Inorg. Chem*., 2006, **45**, 8273.

[57] K. Hu, H.A. Severin, B.D. Koivisto, K.C.D. Robson, E. Schott, R. Arratia-Perez, G.J. Meyer, C.P. Berlinguette, *J. Phys. Chem. C*., 2014, **118**, 17079

[58] L. V. Interrante, G. V. Nelson, *Inorg. Chem*., 1968, **7**, 2059

[59] A. Kumar, S. Sun, J.A. Lees, *Organomet. Chem*., 2010, **29**, 1.

[60] S. García-Fontán, A. Marchi, L. Marvelli, R. Rossi, S. Antoniutti, G. Albertin, *J. Chem. Soc. Dalton Trans*. 1996, 2779

[61] A. Carreño, R. Arratia-Perez, E. Molins, Private Communication, CCDC 1448327

[62] Y. Chen, L. Zhang, Z. Chen, *Acta Cryst*. 2003, **E59**, m429

[63] C. Liu, K. D. Dubois, M. E. Louis, A. S. Vorushilov, G. Li, *ACS Catal.,* 2013, **3**, 655

[64] B. S. Uppal, R. K. Booth, N. Ali, C. Lockwood, C. R. Rice, P. I.P. Elliott, *Dalton Trans.*, 2011, **40**, 7610

[65] C. Redshaw, S. Watkins, S. M. Humphrey, P. C. Bulman Page, S. Ashby, Y. Chao, C. J. Herbert, A. Mueller, *RSC Adv*., 2013, **3**, 23963

[66] G. Parkin, *Chem. Rev*. 1993, **93**, 887

[67] D.H. Waldeck, *Chem. Rev*. 1991, 415.

[68] T. Liu, B. H. Xia, X. Zhou, H. X. Zhang, Q. J. Pan, J. S. Gao, Organometallics, 2007, 26, 143.

[69] W. Herzog, C. Bronner, S. Loffler, B. He, D. Kratzert, D. Stalke, A. Hauser, O.S. Wenger, *ChemPhysChem*, 2013, **14**, 1168

[70] O.S. Wenger, *Coordination Chemistry Reviews*, 2015, **282**, 150

[71] M.T. Zhang, T. Irebo, O. Johansson, L. Hammarstrom, *J. Am. Chem. Soc*., 2011, **133**, 13224

[72] R. Czerwieniec, A. Kapturkiewicz, J. Lipkowski, J. Nowacki, *Inorganica Chimica Acta*, 2005, **358**, 2701

[73] G. F. Manbeck, J. T. Muckerman, D. J. Szalda, Y. Himeda, E. Fujita, *J. Phys. Chem. B*, DOI:10.1021/jp511131x

[74] S.T. Lam, N. Zhu, V. Ka-Man Au, V. Wing-Wah Yam, *Polyhedron*, 2015, **86**, 10

[75] C. Ko, A. W.Y. Cheung, S. M. Yiu, *Polyhedron*, 2015, **86**, 17

[76] P. J. Wright, M. G. Affleck, S. Muzzioli, B. W. Skelton, P. Raiteri, D. S. Silvester, S. Stagni, M. Massi, *Organometallics*, 2013, **32**, 3728.

[77] T. Morimoto, M. Ito, K. Koike, T. Kojima, T. Ozeki, O. Ishitani, *Chem. Eur. J*., 2012, **18**, 3292.

[78] C. Bruckmeier, M.W. Lehenmeier, R. Reithmeier, B. Rieger, J. Herranz, C. Kavakli, *Dalton Transactions*, 2012, **41**, 5026.

[79] Q. Zeng, M. Messaoudani, A. Vlcek Jr, F. Hartl, *Eur. J. Inorg. Chem*, 2012, 471.

[80] M.W. Louie, H.W. Liu, M.H.Ch. Lam, T.Ch. Lau , K.K.W. Lo, *Organometallics*, 2009, **28**, 4297.

[81] G.A. Crosby, J.N. Demas, *J. Phys. Chem*., 1971, **75**, 991

[82] J. Parras-Rojas ; A.A. Moreno ; I. Mitina ; A. Orellana ; *Plos One*, 2015, **10**, 1

[83] P. Staib ; M. Kretschmar ; T. Nichterlein ; H. Hof ; J. Morschhauser ; *PNAS*, 2000, **97**, 6102

[84] C. van Haaften ; A. Boot ; W.E. Corver ; J.D.H. van Eendenburg ; B. J.M.Z. Trimbos ; T. van Wezel ; *Journal of Experimental & Clinical Cancer Research*, 2015, **34**, 38

[85] G. Huang; *Fungal Genom Biol*. 2013, **3**, 1

[86] J.B. Kaper; J.P. Nataro; H.L.T. Mobley; *Nature review; Microbiology*, 2004, **2**, 122

[87] A. Lischewski; M. Kretschmar; H. Hof; R. Amann; J. Hacker; J. Morschhauser; *Journal of Clinical Microbiology*, 1997, **35**, 2943

[88] M.R. Gill, D. Cecchin, M.G. Walker, R.S. Mulla, G. Battaglia, C. Smythe, J.A. Thomas, *Chem. Sci.*, 2013, **4**, 4512.

[89] V. Fernandez-Moreira, I. Marzo, M. Concepcion Gimeno, *Chem. Sci*., 2014, **5**, 4434.

[90] M. L. Bowen, Z.F. Chen, A. M. Roos, R. Misri, U. Hafeli, M. J. Adam, C. Orvig, *Dalton Trans*., 2009, 9228.

[91] R. Yuste, *Imagin: a Laboratory Manual*, Cold Spring Harbor, NY, USA, 2010.

[92] B. Chazotte, *Labeling Nuclear DNA Using DAPI*, Cold Spring Harb Protoc, 2011

[93] H. Lee, J. Kim, H. Kim, Y. Kim, Y. Choi, *Chem. Commun.*, 2014, **50**, 7507

[94] J. Parras-Rojas ; A.A. Moreno ; I. Mitina ; A. Orellana ; *Plos One*, 2015, **10**, 1

[95] P. Staib ; M. Kretschmar ; T. Nichterlein ; H. Hof ; J. Morschhauser ; *PNAS*, 2000, **97**, 6102

[96] C. van Haaften ; A. Boot ; W.E. Corver ; J.D.H. van Eendenburg ; B. J.M.Z. Trimbos ; T. van Wezel ; *Journal of Experimental & Clinical Cancer Research*, 2015, **34**, 38

[97] G. Huang; *Fungal Genom Biol*. 2013, **3**, 1

[98] J.B. Kaper; J.P. Nataro; H.L.T. Mobley; *Nature review; Microbiology*, 2004, **2**, 122

[99] A. Lischewski; M. Kretschmar; H. Hof; R. Amann; J. Hacker; J. Morschhauser; *Journal of Clinical Microbiology*, 1997, **35**, 2943.

[100] G. Repetto; A. del Peso; J.L. Zurita; *Nat. Protoc.* 2008, **3**, 1125

[101] G. Gasser; A. M. Sosniak; N. Metzler-Nolte; *Dalton Trans*. 2011, **40**, 7061

[102] S. I. Kirin; I. Ott; R. Gust; W. Mier; T. Weyhermueller; N. Metzler-Nolte; *Angew. Chem., Int. Ed*., 2008, **47**, 955

[103] V. Márquez-Miranda; J.P. Peñaloza; I. Araya-Durán I, et al. *Nanoscale Research Letters*. 2016, **11**, 66

[104] A. Carreño; S. Ladeira; A. Castel; A. vega; I. Chavez; Acta Cryst. 2012, **E68**, o2507

[105] R. J. Shaver, D. P. Rillema, *Inorg. Chem*, 1992, **31**, 4101

[106] R. Argazzi, C.A. Bignozzi, T.A. Heimer, F.N. Castellano, G.J. Meyer, *Inorg. Chem*., 1994, **33**, 5741

[107] G. B. Blakney, W. F. Allen, *Inorg. Chem.* 1971, **10**, 2763

[108] L. Pazderski, T. Pawlak, J. Sitkowski, L. Kozerskib, E. Szlyk, *Magn. Reson. Chem*., 2010, **48**, 450.

[109] D.J. Stufkens, A. Vlcek, *Coord. Chem. Rev*, 1998, **177**, 127.

[110] K. W. Lee; J. D. Slinker; A. A. Gorodetsky;S. Flores-Torres; H. D. Abrun; P. L. Houston; G. G. Malliaras; PCCP, 2003, **5**, 2706

[111] K. Nakamaru, *Bull. Chem. Soc. Jpn*., 1982, **55**, 1639

[112] M. Kuss-Petermann, H. Wolf, D. Stalke, O.S. Wenger, *J. Am. Chem. Soc.*, 2012, **134**, 12844

[113] G.F. Moore, M. Hambourger, M. Gervaldo, O.G. Poluektov, T. Rajh, D. Gust, T.A. Moore, A.L. Moore, *J. Am. Chem. Soc*., 2008, **130**, 10466

[114] A.A. Pizano, J.L. Yang, D.G. Nocera, *Chem. Sci*, 2012, **3**, 2457

[115] K. Ferreira-Paim; L: Andrade-Silva ; D.J. Mora; E. Lages-Silva; A.L. Pedrosa; P.R. da Silva et al., M*ycopathologia*. 2012, **174**, 41

Fluorescence probes for both prokaryotic and eukaryotic cells using new Rhenium (I) tricarbonyl complexes with an electron withdrawing ancillary ligand †

Alexander Carreño[1,2*], Manuel Gacitúa[3], Juan A. Fuentes[4**], Dayán Páez-Hernández[1,2], Carolina Otero[5], Juan P. Peñaloza[5], Marcelo Preite[6], Elies Molins[7], Wesley B. Swords[8], Gerald J. Meyer[8], Juan Manuel Manríquez [9,2] ,Rubén Polanco[10], Ivonne Chávez[11,2], Ramiro Arratia-Pérez[1,2]

$Re(CO)_3^+$ complexes with an ancillary ligand that presents an electron withdrawing effect suitable for cells imaging.